Spectroscopic investigation of Λ hypernuclei in the wide mass region using the (e,e'K^+) reaction

(Extension request of the currently running E01-011 experiment)

O. Hashimoto (Spokesperson)*, S.N. Nakamura (Spokesperson), Y. Fujii, M. Kaneta, M. Sumihama, H. Tamura, K. Maeda, H. Kanda, Y. Okayasu, K. Tsukada, A. Matsumura, K. Nonaka, D. Kawama, N. Maruyama, Y. Miyagi

Department of Physics, Tohoku University, Sendai, 980-8578, Japan

S. Kato

Department of Physics, Yamagata University, Yamagata, 990-8560, Japan

T. Takahashi, Y. Sato, H. Noumi

Institute for Particle and Nuclear Physics, KEK, Tsukuba, 305-0801, Japan

T. Motoba

Laboratory of Physics, Osaka Electro-Communication University, Neyagawa, 572-8530, Japan

L. Tang (Spokesperson), O.K. Baker, M. Christy, L. Cole, P. Gueye, C. Jayalath, C. Keppel, S. Malace, E.K. Sebefia, V. Tvaskis, L. Yuan

Department of Physics, Hampton University, Hampton, VA 23668, USA

J. Reinhold (Spokesperson), P. Markowitz, B. Beckford, B. Raue, W. Boeglin, L. Kramer, A. Acha, P. Baturin

Department of Physics, Florida International University, Miami, FL 27411 USA

Ed.V. Hungerford, K. Lan, N. Elhayari, N. Klantrains, Y. Li, S. Radeniya

Department of Physics, University of Houston, Houston, TX 77204 USA

P. Bosted, R. Carlini, V.Dharmawardane, R. Ent, H. Fenker, D. Gaskell, M. Jones, D. Mack, J. Roche, G. Smith, W. Vulcan, S.A. Wood, C. Yan

Thomas Jefferson National Accelerator Facility, Newport News, VA 23606 USA

N. Simicevic, S. Wells

Department of Physics, Louisiana Tech University, Ruston, LA 71272 USA

X. Chen, B. Hu, S. Hu, Y. Song. W. Luo, B. Wang

Nuclear Physics Institute, Lanzhou University, Gansu, China

L. Gan

Department of Physics, University of North Carolina at Wilmington, Wilmington, NC 28403 USA

A. Ahmidouch, S. Danagoulian, A. Gasparian

Department of Physics, North Carolina A& T State University, Greensboro, NC 27411 USA

M. Elaasar

Department of Physics, Southern University at New Orleans, New Orleans, LA 70126, USA

R. Asaturyan, H. Mkrtchyan, A. Margaryan, S. Stepanyan, V. Tadevosyan

Yerevan Physics Institute, Armenia

D. Androic, T. Petkovic, M. Planinic, M. Furic, T. Seva

University of Zagreb, Croatia

F. Benmokhtar, T. Horn

Department of Physics, University of Maryland, MD 20742, USA

Ed.F. Gibson

Physics and Astronomy Department, California State University, CA 90840 USA

M. Ahmed

Triangle Universities Nuclear Lab, Duke University, Durham, NC 27708-0308, USA

June 27, 2005

*** Contact person**

Osamu Hashimoto

Department of Physics, Tohoku University, Sendai, 980-8578, Japan
hashimot@lambda.phys.tohoku.ac.jp
Telephone 81-22-795-6452, Fax 81-22-795-6455

Proposal to JLAB PAC-28

Abstract

This proposal is an extension request of the partially approved proposal of JLab E01-011. The experimental goal of the E01-011 experiment was to prove the effectiveness of (e, e'K^+) hypernuclear spectroscopy by employing the "tilt method" for the electron arm and by installing a new high-resolution kaon spectrometer (HKS) for the kaon arm. It was intended to perform a spectroscopic study of Λ hypernuclei for the wide mass region using the (e, e'K^+) reaction, particularly beyond the p-shell region.

The E01-011 experiment is on the commissioning stage in Hall C when this proposal is submitted. Considering the present status of the E01-011 experiment, we are now confident that we can extend the (e, e'K^+) hypernuclear spectroscopic study toward medium-heavy Λ hypernuclei.

The expected results from the proposed experiment will provide Λ hypernuclear excitation spectra with the best energy resolution ever achieved in the reaction spectroscopy. An energy resolution of a few hundred keV and high statistical accuracy of the obtained spectra will clarify the single-particle behavior of a Λ hyperon in a medium-mass nuclear system. These high-quality data will greatly stimulate investigation of baryonic many-body system which has strangeness degree of freedom, the effective Λ-N interaction and ls splitting in the heavier hypernuclei beyond the p-shell. The experiment will take full advantage of high quality electron beam only available at JLab.

The (e, e'K^+) reaction has unique characteristics as outlined below:

- A proton is converted to a Λ hyperon.
- Spin-stretched states are populated with both spin-flip and spin-non-flip amplitudes.
- Reaction spectroscopy with resolution as good as 300 keV (FWHM) can be realized.

The proposed experiment has two goals:

1. Excitation spectra of medium-heavy Λ hypernuclei will be studied using the ^{51}V(e,e'K$^+$)$^{51}_{\Lambda}$Ti reaction, following the ^{28}Si(e,e'K$^+$)$^{28}_{\Lambda}$Al reaction to be studied in the running E01-011 experiment. These spectra will provide precision binding energies and widths for the Λ hyperon in various orbits in the nuclear masses up to $A = 89$. The

new structures and spin-orbit splittings suggested by the recent (π^+, K^+) reaction spectrum in the medium-heavy hypernuclei can be also investigated with unprecedented energy resolution. The present proposal requests additional beam time for exploratory (e,e'K^+) spectroscopy for the ^{89}Y(e,e'K^+)$^{89}_{\Lambda}$Sr reaction, too.

2. Excited states of neutron rich p-shell hypernuclei, will be systematically investigated, employing enriched isotope targets of ^{6,7}Li, ^{10,11}B targets. It provides essential data to shed lights on the controversial $\Lambda - \Sigma$ coupling strength, which is supposed to play an important role in the interior of neutron stars.
   It is emphasized that the present program also lays the foundation for multi-strangeness nuclear physics, which requires reliable information on ΛN interactions through the structure of Λ hypernuclei.

The proposed experimental geometry with "tilt method" greatly reduces the bremsstrahlung count-rate in the electron spectrometer, and allows us to take data with a 30 μA electron beam and 100 mg/cm^2 thick target. In order to further increase the hypernuclear yield rates and improve the resolution, a new high-resolution, large-acceptance kaon spectrometer (HKS) has been installed in the E01-011 experiment and in operation, replacing the SOS spectrometer which was used in E89-009. We will fully use the HKS spectrometer for the proposing experiment. In addition, a new high-resolution electron spectrometer (HES) and a new splitter magnet are under construction by the collaboration. With the HES which can analyze electron momentum as high as 1 GeV/c, we are able to run under 6 GeV and 12 GeV operation since we can accept 2.1 - 2.5 GeV primary electron beams.

Either the existing ENGE spectrometer or the new HES spectrometer will be employed as an electron spectrometer depending on the available beam energy, though the HES spectrometer is not ready before the end of 2006.

The proposed experiment aims to further extend the series of hypernuclear studies at JLab, E89-009 and E01-011 in Hall C and E94-107 in Hall A, and will firmly establish (e,e'K^+) spectroscopy which is essential for the investigation of hadronic many-body systems with strangeness.

1 Physics Motivation and Experimental Objectives

1.1 Significance of hypernuclear investigation

Hypernuclear investigations provide invaluable information on many-body hadronic systems. Both structure of baryons in the nuclear medium and structure of nuclei as baryonic many-body system can be better studied by introducing a "strangeness" degree of freedom into a nucleus [1, 2, 3, 4]. In particular, a Λ hyperon can be put deep inside a nucleus as an impurity and provides a unique and sensitive probe of the nuclear interior.

It is not straightforward to investigate the interior of a nucleus or deeply bound nuclear states using traditional experimental techniques. In principle, nucleon knockout reactions such as (e,e'p) and (p,2p) can reveal the single-particle aspects of the deeply bound states. However, the nuclear deeply bound states get broader for deeper bound states, and thus the precision spectroscopic investigation is impossible. For example, the spreading widths reach 5 MeV for the $1f$ shell proton states of ^{208}Pb.

Since the Λ hyperon does not suffer from Pauli blocking by the other nucleons, it can penetrate into the nuclear interior and form deeply bound hypernuclear states. It is expected that new forms of hadronic many-body systems can be investigated using this new degree of freedom, "strangeness", and also comparing the hyperon-nucleon and nucleon-nucleon interactions. New nuclear structure, which cannot be seen in ordinary nuclei consisting only of nucleons, can manifest itself in hypernuclei, providing indispensable information on flavor SU(3) baryonic many-body system.

Furthermore, hyperon-nucleon (YN) and hyperon-hyperon (YY) interactions can be well studied by the spectroscopic investigation of hypernuclei. Hyperon-nucleon scattering experiments are supposed to provide basic data on the interactions but it is quite difficult to carry out such experiments, because hyperon lifetimes are quite short (of the order of 10^{-10} s) and hyperon beams suitable for the scattering experiments are not readily available. Spectroscopic investigations yield valuable information on the hyperon-nucleon and hyperon-hyperon interactions.

Assuming a Λ hypernuclear wavefunction is decomposed into a core nucleus and a Λ hyperon, the hypernuclear Hamiltonian is expressed as

$$H = H_{Core\ Nucleus} + t_\Lambda + \sum v_{\Lambda N}^{effective}, \tag{1}$$

where $H_{Core\,Nucleus}$ is the Hamiltonian for the core nucleus, t_Λ is the kinetic energy of the Λ hyperon and $v_{\Lambda N}^{effective}$ describes the effective ΛN interaction. The effective interaction can be constructed with using the G-matrix calculation, from the two-body interactions in free space. One-boson-exchange models such as Nijmegen [5] and Jülich interactions [6] (which were constructed by extending NN interaction models on the basis of flavor SU(3) symmetry with scarce ΛN and ΣN scattering data used to adjust parameters) are widely used to describe the elementary two-body interactions.

Analytical forms of the effective potentials are often given in the form of a three-range gaussian, $V_{\Lambda N}(r) = \sum_i (a_i + b_i k_f + c_i k_f^2) \exp(-r^2/\beta_i^2)$ [7]. A wide variety of hypernuclear properties such as level structure and reaction cross sections are calculated using this potential and compared directly with the experimental data. These calculations are reasonably reliable, in part, because the ΛN interaction is much weaker than the NN interaction and no anti-symmetrization against nucleons is required.

Furthermore, it should be noted that the recent progress of theoretical studies on few-body hypernuclei allows us to calculate the binding energies of ground and excited states for lighter systems directly from free two-body interactions. Those calculation can be compared with the high accuracy experimental data. In such studies, information on Λ hypernuclear structure obtained by spectroscopic studies plays an essential role in testing and improving YN interaction models. Quantitative understanding of YN and YY interactions is a key issue for investigation of the new aspects and new forms of hadronic matter. In particular, detailed information on YN and YY interactions is indispensable for our understanding of high-density nuclear matter inside neutron stars, where hyperons are possibly mixed and playing crucial roles.

A Λ hypernucleus is produced in a wide variety of hadronic reactions with beams of mesons, protons, and heavy-ions. It can be also produced by electromagnetic interactions, though an experimental technique became feasible quite recently. In most cases of hypernuclear reactions, a hypernucleus is populated in a nucleon-hole hyperon-particle state (a nucleon in the target having been converted to a Λ hyperon). From a view point of constituent quarks, an s quark in the beam kaon is exchanged with a d quark in a neutron in the case of the (K^-, π^-) reaction, while in the (π^+, K^+) reaction and also in the (e, e'K^+) reaction, an s-$\overline{s}$ pair is created associatively, resulting in the production of both a Λ hyperon and a kaon.

Once a Λ hypernucleus is produced in an excited state, it decays through strong, electromagnetic and weak interactions according to the nature of the states, as shown pictorially in Fig. 1.

The Λ binding energies are usually much larger than those for a proton or a neutron. The hypernuclear states with an orbit above the p-shell in which a Λ hyperon is bound, are often nucleon unbound and decay by emitting nucleons. Even for high-lying Λ hypernuclear states above the nucleon emission thresholds, the calculated spreading widths are narrower than a few 100 keV, in marked contrast to the case of an ordinary nucleus [8, 9]. This is because, (1) ΛN interaction is weaker than the nucleon-nucleon interaction, (2) ΛN spin-spin interaction is weak and therefore spin vector p_N-h_N excitation is suppressed, (3) a Λ hyperon with zero isospin can excite only isoscaler p_N-h_N modes of the core nucleus, and (4) no exchange term with nucleons is required. These characteristics make the widths of Λ hypernuclear states considerably narrower than states in an ordinary nucleus with a similar excitation energy. In the case of Ca, for example, Bando *et al.* predicted that $\Gamma_\Lambda(1s,0d)/\Gamma_N(0s) = 0.03 - 0.07$. The widths are expected much smaller than the energy spacings between the Λ major shells and, consequently, Λ hypernuclear states should be observable as reasonably narrow peaks. This provides a basis for reaction spectroscopy of Λ hypernuclei with resolution as good as a few 100 keV for a wide range of excitation.

When Λ hypernuclear states below the particle emission threshold are populated either directly by the reaction or indirectly after de-excitation, γ transitions take place down to the hypernuclear ground state, which eventually decays through weak interaction (see Fig. 1).

In the investigation of hadronic many-body system with strangeness, there is a fundamental question, "to what extent does a Λ hyperon keep its identity as a baryon inside a nucleus?" [10]. Spectroscopic data in heavier hypernuclei can help to answer this question. Indeed, the relevance of the mean-field approximation in nuclear physics is one of the prime questions related to role that the sub-structure of nucleons plays in the nucleus.

Hypernuclear spectroscopy is quite powerful tool for the quantitative investigation of these basic questions of hadronic many-body systems.

1.2 Recent experimental investigation of Λ hypernuclei

Λ hypernuclear investigation has already undergone half a century since the first discovery of the hypernucleus in 1953 [11]. Although the spectra of many light Λ hypernuclei have been studied primarily using hadronic reactions, there are only a few experiments on hypernuclear systems beyond the p-shell region.

Most of data for heavy Λ hypernuclei were obtained using the (π^+, K^+) reaction, which preferentially populates deeply-bound, high-spin states because a large momentum is transfered to the recoil hypernucleus in this reaction. The BNL-AGS experiments surveyed the single particle nature of Λ hypernuclei up to ${}^{89}_{\Lambda}$Y, and observed peaks corresponding to the major Λ shell structure [12]. The KEK E140a experiment made an intensive spectroscopic study using the SKS spectrometer [13, 14], and observed the major shell structure of the single particle Λ orbits up to ${}^{208}_{\Lambda}$Pb [15, 16]. These spectra, shown in Fig. 2, were interpreted in terms of a Λ bound in a Woods-Saxon, density-dependent potential. However, the spectra are too poor quality as seen in Fig. 2, to determine confidently the peak positions of the various shell structures. Resolutions varied from 1.5 to 4 MeV FWHM from the light to heavy systems.

The best hypernuclear spectrum in the medium-heavy mass region so far was taken for the ${}^{51}_{\Lambda}$V and ${}^{89}_{\Lambda}$Y by the (π^+, K^+) reaction with an energy resolution of 1.7 MeV (FWHM) as shown in Figs. 3,4 [17, 18].

For ${}^{89}_{\Lambda}$Y, a series of bumps observed in the spectrum reflects the coupling of a Λ hyperon in the major orbits to the $0g^{-1}_{9/2}$ neutron-hole state of the ^{88}Y core. As noted above, the widths of the states corresponding to the p, d, and f-orbits were significantly broader than the experimental resolution of the ${}^{89}_{\Lambda}$Y spectrum as estimated from the resolution of the ${}^{12}_{\Lambda}$C spectrum and energy loss straggling of pions and kaons in the target. Assuming that the experimental resolution is 1.65 MeV FWHM for all peaks, each bump structure was interpreted as corresponding to a major shell but split to two peaks [17]. There are two possible explanations for the apparent splitting of the major shell bumps. One is the interplay of core excited states due to different holes for the neutron orbits, and the second is ls splitting of the high-l Λ orbits [17]. If the observed splitting is attributed solely to the ls splitting, the ls interaction in ${}^{89}_{\Lambda}$Y is much larger than that observed in light Λ hypernuclear data, particularly the recent γ-ray measurements [19, 20]. Motoba pointed out that the intensity ratios

between the split two peaks should be less than unity if the two peaks are ls partners, but the experimental result gave the ratios greater than unity. An intensive calculation taking into account the configurations of $0g_{9/2}, 2p_{1/2}, 2p_{3/2}, 0f_{5/2}, 0f_{7/2}$ and sd neutron hole states was recently carried out. It was reported that the calculated spectrum accounted for the experimental spectrum without assuming large ls splitting [21], but it is still an open question. The $^{51}_{\Lambda}$V spectrum given in Fig. 4 also shows similar structure.

Considering these results, it is clear that full understanding of the spectral shapes of the heavy Λ hypernuclei requires experimentally much better energy resolution and theoretically proper consideration of core excitation and mixing of different parity states, since it becomes easier to excite the various states of the core nucleus in heavy hypernuclei. Therefore, high-resolution high-quality spectroscopy is eagerly waited.

For p-shell Λ hypernuclei, good resolution hypernuclear spectra were measured again by the (π^+, K^+) reaction at KEK PS and the structure information on light Λ hypernuclei were obtained [22]. The spectra yielded information on the hypernuclear structure such as core excited states and also on spin-dependent ΛN interaction. A sample spectrum for the ^{12}C(π^+,K$^+$) reaction is shown in Fig. 5.

Other striking progress in hypernuclear spectroscopy involves the observation of γ transitions between hypernuclear states which are excited by pion or kaon production reactions, although γ-ray spectroscopy is applicable only to the states below particle emission threshold. The γ rays are recently observed by Germanium and NaI detectors in coincidence with the production of bound hypernuclear states. With energy resolution as low as a few keV (FWHM), γ-ray spectroscopy has succeeded in obtaining the strengths of spin-dependent Λ-nucleon interactions in p-shell Λ hypernuclei through the observation of small splittings due to the spin-dependent interactions in $^{7}_{\Lambda}$Li [23], $^{13}_{\Lambda}$C [24], $^{9}_{\Lambda}$Be[25] and $^{16}_{\Lambda}$O [26].

For reaction spectroscopy, with which one can study hypernuclear states even above the particle emission thresholds, the best energy resolution achieved so far is 1.45 MeV (FWHM) by the (π^+, K^+) reaction. The resolution is governed by the beam quality and target thickness for reaction spectroscopy using the secondary beams such as pions and kaons. On the other hand, (e, e'K$^+$) reaction spectroscopy, with the high-quality primary beam, can overcome such inherent difficulty of (π^+, K^+) and (K^-, π^-) reaction spectroscopy for achieving sub-MeV mass resolution.

The series of (e, e'K^+) hypernuclear spectroscopy experiments has been highly motivated by the potential of its high resolution spectroscopy, which is expected to plays an essential role in the qualitative investigation of hadronic many-body system with strangeness.

The present issues in hypernuclear spectroscopy can be summarized in the following two points,

- To what extent the single-particle properties of a baryon persisted in deeply bound states. This can be studied by placing a Λ hyperon deeply within the nucleus.
- What is the shape and strengths of the effective Λ-Nucleus potential and also the spin dependent interaction strengths,

Although the spin-dependent interaction can be precisely studied in the p-shell by γ-ray spectroscopy, complementary information from higher mass nuclei and higher excitation energies is equally important. Furthermore, the single particle nature of the Λ hyperon embedded in nuclear matter can be studied only by spectroscopy of heavy hypernuclei, and this is the key motivation of this proposal.

1.3 Experimental objectives

The partially approved E01-011 experiment intended to establish high-precision spectroscopy of Λ hypernuclei by the (e,e'K^+) reaction for the wide mass range. However, the beam time was approved only for the first two proposed targets, ^{12}C and ^{28}Si. Now that the new high resolution, large solid-angle kaon spectrometer system (HKS) has been successfully installed in Hall C and the E01-011 commissioning is underway, we propose to extend the program to heavier targets as we previously proposed, and also to lighter p-shell targets.

The experimental objectives of this extension proposal are summarized below.

1. Spectroscopy of medium-heavy Λ hypernuclei
   (a) We plan to measure high-precision binding energies of Λ single particle states with various l from the excitation spectra of Λ hypernuclei up to A=51 region and also an exploratory experiment in the A=89 region.

The limited resolution of the (π^+, K^+) reaction makes it difficult to extract precise Λ binding energies except for the light Λ hypernuclei. Energy resolutions of a few 100 keV, which is comparable to the spreading widths of excited hypernuclear states, are needed to extract these binding energies. This information provides the depth of the central potential and possible spin-orbit splittings over a wide mass region. The mass dependence of the single particle levels can be directly compared to calculations using single particle potentials and recent mean-field theory. Since p-orbits of a Λ hyperon are barely bound in the p-shell Λ hypernuclei, it is essential to extend this measurement to heavier systems. The proposed experiment also provides information on the widths of these single particle orbits.

Effective masses of a Λ hyperon in the nuclear potential will be obtained from the binding energies of a Λ hyperon in various l orbits. The effective mass is expected to be closer to that of its free value in contrast to the case of ordinary nuclei. Therefore, the proposed precision measurement of the single particle levels can address the degree of non-locality of the effective Λ-Nucleus potential and also can be compared, for example, with the advanced mean field calculations based on quark-meson coupling (QMC) model [27]. This can be related to the nature of the ΛN and ΛNN interactions, and to the ΛN short range interactions [33].

In a more exotic way, the binding energies were discussed in terms of the distinguishability of a Λ hyperon in nuclear medium, which will result in different A dependence of the binding energy as suggested by Dover [28].

(b) We will also study unique structure of medium-heavy Λ hypernuclei and possibly spin-orbit splitting of the Λ single particle states in these hypernuclei. As previously discussed, the ^{89}Y spectrum taken by the (π^+, K^+) reaction shows that the higher l states are split by about 1 MeV. It was suggested that these splittings are due to the ΛN ls interaction, although the magnitude of the splitting is much larger than expected from previous measurements in the p-shell region, and, in particular, from the recent γ ray data of $^{9}_{\Lambda}$Be. The observed splittings were

also interpreted as due to an interplay of different neutron hole states. With the resolution of 3-400 keV, we will disentangle closely degenerate hypernuclear states, and clarify the origin of the splittings. If the origin of the splitting is due to ls interaction, we will learn the magnitude of the interaction from it. In this case, the result will introduce a deeper puzzle about the changes of the ls strength from the p-shell region Λ hypernuclei to the medium-heavy Λ hypernuclei. In other cases if the splitting is due to the core excitation, it will give us information on the characteristic hypernuclear structure of medium-heavy hypernuclei. In either case, new features of Λ hypernuclei will be investigated by the precise (e, e'K^+) hypernuclear spectroscopy.

2. Spectroscopy of p-shell hypernuclei

   We also propose to investigate the structure of p-shell hypernuclei systematically for ${}^{6,7}_{\Lambda}$He and ${}^{10,11}_{\Lambda}$Be with ^{6,7}Li and ^{10,11}B target, respectively. It is particularly important to study these hypernuclei with enriched targets and obtain information on the isospin dependence of the structure. Such data are now expected to shed lights on $\Lambda - \Sigma$ coupling, as the isospin plays crucial role [29]. Recent theoretical investigation claims that the $\Lambda - \Sigma$ coupling should be properly taken into account to clarify the dynamics of interior of neutron stars.

2 The (e, e'K^+) reaction for the hypernuclear spectroscopy

2.1 Hypernuclear production reactions

The (e, e'K^+) reaction has a unique characteristics for hypernuclear spectroscopy among a wide variety of reactions which can be used to produce a strangeness -1 hyperon as listed in Table 1. Each reaction has its own characteristics and plays its role for Λ hypernuclear spectroscopy. So far, only the (K^-, π^-) and (π^+, K^+) reactions have been intensively used for the spectroscopic investigation among these reactions; these reactions convert a neutron in the target nucleus to a Λ hyperon. Although the (π^+, K^+) reaction is relatively new compared to the (K^-, π^-) reaction, it is now considered as one of the best reactions for hypernuclear spectroscopy

Table 1: Comparison of Λ Hypernuclear production reactions

ΔZ = 0 *neutron to* Λ	ΔZ = -1 *proton to* Λ	comment
(π^+, K^+)	(π^-, K^0)	stretched,high spin
in-flight (K^-, π^-) stopped (K^-, π^-)	in-flight (K^-, π^0) stopped (K^-, π^0)	substitutional
$(e, e'K^0)$ (γ, K^0)	$(e, e'K^+)$ (γ, K^+)	spin-flip,unnatural parity

because it favorably populates deeply bound hypernuclear states [12, 15, 30]. The smaller cross sections of the (π^+,K$^+$) reaction compared to that of the (K$^-$,π^-) reaction are compensated by the intensity of pion beams, which is much higher than that of kaon beams. The (π^+,K$^+$) reaction selectively populates angular momentum stretched states because of the large momentum transfer to the recoil hypernuclei [31, 32, 33]. This is in contrast to the (K^-, π^-) reaction, which transfers small momentum and thus preferentially excites substitutional states. By high quality (π^+, K^+) spectra with resolution better than 2 MeV (FWHM), it became possible to populate deeply bound Λ states, and to study qualitatively the unique structure of Λ hypernuclei and characteristics of the Λ-nucleon interaction.

2.2 The (e,e'K$^+$) reaction

Since the momentum transfer of the (e,e'K$^+$) reaction is almost the same as that of the (π^+, K^+) reaction, it is expected to preferentially populate high-spin bound hypernuclear states similarly to the (π^+, K^+) reaction (Fig. 6). However, in contrast to the reactions with meson beams, the (e, e'K$^+$) reaction will populate spin-flip hypernuclear states as well as non-spin-flip states, since the transition operator has spin-independent (f) and spin-dependent (g) terms [34, 35].

Another characteristics of the (e,e'K$^+$) reaction is that it converts a proton to a Λ hyperon, in contrast to the (π^+, K^+) and (K^-, π^-) reactions. This results in proton-hole-Λ-particle states in the configuration $[(lj)_N^{-1}(lk)^\Lambda]_J$. When the proton hole state is $j_> = l + 1/2$, the highest spin states of $J = J_{max} = j_> + j_>^\Lambda = l_N + l_\Lambda + 1$ are favorably excited. These

hypernuclear states are of unnatural parity when the original proton orbit is $j_>$. On the other hand, if the hole state has spin $j = j_< = l - 1/2$, the highest spin states of the multiplet $J'_{max} = j_< + j^\Lambda_> = l_N + l_\Lambda$ with natural parity are strongly populated. This selectivity is particularly important as it allows us to directly study the spin-dependent structure of Λ hypernuclei.

Experimentally, the most important characteristics of the (e,e'K^+) reaction is that it can potentially achieve significantly better energy resolution because the reaction is initiated with a primary electron beam. The beam emittance and the energy spread are extreme good compared with the secondary meson beams. If high performance spectrometers are available for scattered electrons and kaons, energy resolution of a few 100 keV can be achieved.

The unique characteristics of the (e,e'K^+) reaction are summarized below.

- Extremely good energy resolution when coupled with the high resolution kaon spectrometer (HKS).
- Production of natural and non-natural parity states.
- Production of neutron rich hypernuclei as the reaction replaces a proton by a Λ.
- Reliable energy scale calibration by the elementary p(e,e'K^+)Λ reaction on a CH_2 target.

Although the (e,e'K^+) reaction has many advantages for hypernuclear spectroscopy, it has not been realized because the cross section is much smaller than reactions using hadronic beams and two high resolution spectrometers are required. For example, the calculated cross section for the ^{12}C(e,e'K^+)$^{12}_\Lambda$B$_{gr}$ is two orders of magnitude smaller than that of the corresponding ^{12}C(π^+,K^+)$^{12}_\Lambda$C$_{gr}$ reaction. Actually hypernuclear yields of the ground state of $^{12}_\Lambda$B with the E89-009 setup are smaller by almost two order of magnitude compared with that of $^{12}_\Lambda$C by the SKS experiment at KEK. However, this disadvantage can be overcome by employing a new geometry which we proposed for the E01-011 experiment and plan to adopt in this proposed experiment. The proposed experimental setup employs a new High resolution Kaon Spectrometer (HKS) and also the "tilt method" for the electron spectrometer as described in the next section.

2.3 Previous (e,e'K+) experiments

The first hypernuclear electro-production experiment has been successfully completed in Hall C at JLab in the spring of 2000. This experiment used the ^{12}C(e,e'K$^+$)$^{12}_{\Lambda}$B reaction, and observed the ground state peak of $^{12}_{\Lambda}$B hypernucleus. The experiment demonstrated that the Λ hypernuclear spectroscopy can be performed by the (e,e'K$^+$) reaction and that sub-MeV energy resolution can be obtained as shown in Fig. 7. The resolution obtained in the experiment, $\sim$750 keV, is better by a factor of 3 than that previously obtained.

The E89-009 experiment was designed to take advantage of the peak in the virtual photon flux at very forward angles. Therefore, it had low luminosity since a maximum number of photons/incident electron were available for reactions. The experimental setup is schematically shown in Fig. 8. Zero degree electrons and positive kaons were bent into their respective spectrometers on opposite sides of the beam by a splitter magnet. The electron momentum was analyzed by a small Split-Pole spectrometer positioned to detect zero degree electrons. Positive kaons were detected also at around 0 degrees using the SOS spectrometer.

The experiment utilized a low beam current of 0.66 μA with a ^{12}C target 20 mg/cm^2 thick.

Although the experiment was successful, the yields were limited due to the background flux of bremsstrahlung electrons in the electron spectrometer. The experiment E89-009 provided valuable information on rates and cross sections in order to design a geometry for E01-011, however, we had recognized that further improvement of experimental configuration is indispensable to extend these studies to heavier systems.

Later in 2004, the E94-107 experiment obtained greatly improved $^{12}_{\Lambda}$B spectrum using the Hall A HRS spectrometers and a septum magnet. The experimental conditions are different from that of E01-011. The measured spectrum for the ^{12}C(e, e'K$^+$)$^{12}_{\Lambda}$B reaction is considerably improved (mass resolution of $\sim$700 keV) from that of E89-009. It is noted that the data were taken with approximately 1 week beam time thanks to an order of magnitude higher yield rate compared with E89-009. The E01-011 experiment expects to accumulate the similar statistics in one day with a 30 μA beam and to achieve twice better mass resolution (300-400 keV).

3 Proposed experiment

3.1 Principle of the proposed experimental

The principle of the proposed experiment is essentially the same as the pioneer (e, e'K^+) hypernuclear spectroscopy E89-009. The improvements of the E01-011 experiment can be summarized as follows.

- A new high resolution kaon spectrometer (HKS) was installed in Hall C; it has 16 msr solid angle combined with the splitter and simultaneously achieves 300-400 keV (FWHM) hypernuclear mass resolution.
- A new experimental configuration will maximize hypernuclear production rates by avoiding the 0-degree bremsstrahlung electrons but still measure scattered electrons at a sufficiently forward angle. With the "tilt method", the electron spectrometer is tilted vertically by a few degrees. Observing the scattered electrons out of the dispersion plane, we can avoid the very forward bremsstrahlung electrons. The "tilt method" allows us to accept a beam current as high as a few tens μA. The tilt angle is optimized for a given experimental kinematics so that bremsstrahlung electrons and Mϕller electrons do not enter the acceptance of the electron arm.

It is emphasized that hypernuclear yield per a certain solid angle is approximately inversely proportional to hypernuclear mass number with the proposed "tilt method", while the bremsstrahlung electron rate in the electron arm, which limited the beam intensity, is roughly proportional to inverse of $Z^{2+\delta}$ when the 0-degree tagging method is employed. The "tilt method" allows us to accept much higher beam currents because the high rate bremsstrahlung electrons are not allowed to enter the ENGE spectrometer.

3.2 Proposed experimental condition

In the proposing experiment, the experimental geometry and conditions are basically the same with those of the currently running E01-011 experiment; the beam energy should be in a range of 1.8-1.9 GeV. However, we are now constructing a new high-resolution electron spectrometer (HES) which accepts higher energy electrons than the ENGE spectrometer does. We will

have capability of accepting wider region of beam energy, once the HES is constructed. In this subsection let us give the general consideration of the experimental conditions. In the following subsection we will present the two spectrometer configurations, 1) ENGE option and 2) HES option, which allow us to carry out the proposed experiment with wider range of beam energy, and thus the constraint on the other halls' energies is more relaxed.

In order to optimize the experimental conditions for high-resolution and high efficiency hypernuclear spectroscopy, the following items are taken into account:

1. For the yield of Λ hypernuclei, three factors contribute:

   (a) The elementary cross section of p(γ,K$^+$)Λ has little energy dependence in the range of real γ from 1.1 to 2.0 GeV. Corresponding kaon momentum is from $\sim$0.7-1.6 GeV/c. However, the hypernuclear production cross sections get greater with the higher γ energy because the recoil momentum becomes smaller.

   (b) With higher kaon momentum, the survival rate of the kaon becomes higher for a given flight path of the spectrometer.

   (c) With a higher kaon momentum, the angular distribution of scattered kaons becomes smaller. Therefore, a larger fraction of the produced hypernuclei will be measured for the same solid angle if the spectrometer is positioned at close to 0 degrees.

   The figure of merit as a function of electron energy with the scattered electron energy of 0.285 GeV, is shown in Fig. 9. It can be seen that the higher the energy of the electron beam gives the larger the yield of the hypernuclear ground states for a given spectrometer configuration.

2. As shown in Fig. 10 and Fig. 11, the angular distributions of virtual photons and kaons in the (e,e'K$^+$) reaction is forward peaked, and thus both the electron and the kaon spectrometer should be positioned at as forward angles as possible. We satisfy this condition by introducing a splitter magnet just downstream of the target position. However, there are two background sources when we measure at very forward electrons associated with hypernuclear production. One is the bremsstrahlung electron and the other Mϕller electron. These

background electrons can be highly suppressed by tilting the scattered electron spectrometer vertically with respect to the dispersive plane defined by the splitter magnet at the cost of hypernuclear yield loss (the "tilt method"). The tilt angle is optimized considering the figure of merit of hypernuclear yield and background rates. In the E01-011 experimental condition, the "tilt method" suppresses background quite efficiently with a reasonable loss of virtual photons which contribute to produce hypernuclei. Highly improved signal-to-noise ratio allows us to increase beam luminosity, and thus hypernuclear yield per a given beam time is expected to increase by a factor of 50.

3. The virtual photons at 0 degrees have the energy, E_γ, and is given as,

$$E_\gamma = E_e - E_{e'} \tag{2}$$

where E_e and $E_{e'}$ are beam and scattered electron energies. The elementary cross section of the (γ,K^+) reaction has relatively weak E_γ dependence above the threshold.

4. Once the central energy of virtual photon is fixed at 1.5 GeV, outcoming K^+ momentum is calculated using the resultant hypernuclear mass. Since the momentum acceptance of the HKS spectrometer is centered at 1.2 GeV/c, the required beam energy is determined once the central energy of the electron arm is given. In the case of E01-011, the central energy of scattered electrons is fixed to be approximately 0.3 GeV as we use the ENGE spectrometer. Therefore the beam energy should be around 1.8 GeV. In order to accept the higher beam energy, the energy range of the electron spectrometer should be higher, requiring a new electron spectrometer.

   Fig. 12 presents the correlation between the electron and kaon momenta for the production of Λs, Σs and the $^{51}_{\Lambda}$Ti hypernucleus states. The E01-011 geometry and also the setup for the present proposed experiment was designed to have a wide mass acceptance. It is vitally important to have acceptance which covers wide mass range so that the mass scale calibration can be properly carried out from the experimental data.

5. We considered following items in the design of HKS to optimize the central kaon momentum:

(a) Yield of hypernuclei.

(b) Energy resolution and acceptance of the spectrometer. Naturally, the energy resolution becomes worse with higher momentum.

(c) Particle identification, particularly between pions and kaons.

(d) Size of the kaon spectrometer and consequently construction cost.

Taking into account above conditions, the optimum kaon momentum was set at 1.2 GeV/c in order to achieve 2×10^{-4} (FWHM) momentum resolution. This momentum resolution corresponds to about 100 keV energy resolution in hypernuclear excitation spectra.

6. Although the hypernuclear yield is expected to increase with higher beam energy, reaction channels producing hyperons other than a Λ hyperon open at higher energy. They can be sources of background, since bremsstrahlung photons can be produced in the targets with an energy of up to the primarily beam energy.

   Our strategy is to keep the electron beam energy low from the points of background from the other reaction channels and also easiness of the particle identification. It also helps to realize the higher momentum resolution of the kaon arm.

7. Matching to the resolution the kaon spectrometer, the electron spectrometer should have good momentum resolution of $\leq 3 \times 10^{-4}$. Since the momentum of scattered electron is lower compared to that of kaons, the absolute momentum resolution can be better.

3.3 Proposed experimental configuration

We propose two configurations for the proposed experiment, taking full advantage of the "tilt method".

A) HKS + ENGE + existing splitter magnet,

B) HKS + HES + new splitter magnet.

The configuration A will use the experimental setup same as E01-011. Since the E01-011 experiment has been running at the time of the proposal submission and all required detectors, resources are ready, we can take data with this geometry anytime in principle. The beam energy is, however,

limited to be around 1.8 GeV as explained in the previous subsection, and thus other halls' beam energies are constrained.

The configuration B requires to introduce a new high-resolution electron spectrometer (HES) which can momentum-analyze electrons as high as 1.0 GeV. However, this configuration B is more flexible and it allows us to accept wider range of electron beam energy, even for the 12 GeV operation. Since we take it granted that the HKS spectrometer is the most optimized one for kaon detection, the range of the beam energy we can accept in the HKS-ENGE combination in E01-011 is narrow as shown in Fig. 13.

As described later, the collaboration has already started the construction of the electron spectrometer (HES) together with a new splitter magnet that matches HES

The HES spectrometer is designed so that the hypernuclear yield rates with the configuration B is equal or larger than that of the configuration A. Therefore, we will present estimates of hypernuclear yield rates mostly for the case of configuration A in this proposal.

The E89-009 experimental setup accepted reaction electrons and kaons at angles down to zero degrees. It was found that the 0-degree electron-tagging method was limited by the accidental rate from bremsstrahlung electrons. We therefore propose to tilt the electron spectrometer by a small angle sufficient to exclude electrons from the bremsstrahlung and Mϕller processes.

A plan view of the proposed geometry, splitter+ENGE spectrometer +high resolution kaon spectrometer (HKS), is shown in Fig. 14. Both the HKS spectrometer and the ENGE spectrometer are positioned as forward in angle as possible, without accepting 0-degree electrons or positrons. The HKS spectrometer, having a QQD configuration, was newly designed for the kaon arm. It has a momentum resolution of 2×10^{-4} (FWHM) at 1.2 GeV/c, and a large solid angle of 16 msr, including the splitter. This is summarized in Table 2.

In designing of the proposed experiment, E89-009 data were fully utilized and singles rates of electrons, positrons, pions and protons in each arm were extracted. These are compared with the EPC code calculations and the normalization factors were derived. Assuming the obtained normalization factor for the hadron production rate at the forward angles, singles rates of the counters in the proposed setup were evaluated.

In the configuration A, the ENGE split-pole spectrometer used for the E89-009 experiment will be adopted for the scattered electrons. However, the spectrometer is to be vertically tilted by about 8 degrees which corresponds to 4.5 degrees of the electron scattering angle, so that the bremsstrahlung / Mϕller electrons do not enter the spectrometer acceptance. The components of the focal plane detector system were redesigned and served in the running E01-011 experiment.

The splitter magnet used in E89-009 was modified to have wider gap so that it matched the HKS geometrical acceptance.

The configuration and specification of the proposed hypernuclear spectrometer system is summarized in Table 2 and is shown in Fig. 14.

Table 2: Experimental condition and specification of the proposed hypernuclear spectrometer system

Beam condition	
Beam energy	1.8 GeV
Beam momentum stability	1×10^{-4}
General configuration	Splitter+HKS spectrometer+ENGE spectrometer
HKS spectrometer	
Configuration	Q-Q-D and horizontal 70° bend
Central momentum	1.2 GeV/c
Dispersion	4.7cm/%
Momentum acceptance	$\pm$ 12.5% (1.05-1.35 GeV/c)
Momentum resolution ($\Delta p/p$)	2×10^{-4}
Solid angle	16 msr with a splitter (30 msr without splitter)
Kaon detection angle	Horizontal : 7 degrees (1-13°)
Flight path length	10 m
Maximum magnetic field	1.6 T (normal conducting magnet)
ENGE split-pole spectrometer	
Central momentum	0.3 GeV/c
Momentum acceptance	$\pm$ 20 %
Momentum resolution ($\delta p/p$)	2×10^{-4}
Electron detection angle	Horizontal : 0 degrees Vertical : 4.5 degrees

3.4 Proposed reactions

1. **p(e,eK$^+$)Λ and ^{12}C(e,e'K$^+$)$^{12}_{\Lambda}$B reactions**

   The p(e,eK$^+$)Λ and ^{12}C(e,e'K$^+$)$^{12}_{\Lambda}$B reactions are used to calibrate the spectrometer system with CH_2 and ^{12}C targets for the absolute missing mass scale. The procedure has been established in the E89-009 and running E01-011 experiments. With the known Λ, Σ, $^{12}_{\Lambda}$B (g.s.) masses, the kaon and electron spectrometer system and primary electron beam energy are calibrated so that the absolute scale of the binding energy can be precisely determined. Since we aim to determine the absolute binding energies of a Λ hyperon in the mass region where no emulsion experiments exist, those reactions are essential for the present experiment. It is in contrast to the (π^+, K^+) reaction in which we have to rely on other indirect reactions since a neutron target is not available.

2. **^{51}V(e,e'K$^+$)$^{51}_{\Lambda}$Ti reaction**

   In the ^{51}V target, the neutron $f_{7/2}$ shell is reasonably well closed and stable because N=28. The reaction is supposed to convert one of the three protons in the f-shell to a Λ hyperon. In this hypernuclear mass region, the Λ hyperon is bound up to the d-orbit, providing us an opportunity to determine the binding energies up to higher l states. The hypernucleus, $^{51}_{\Lambda}$V, was studied by the (π^+, K^+) reaction at KEK-PS. Fig. 3 shows the Λ binding energy spectrum, quality of which is not good enough to separate sub-peaks. However, the major shell structure can be seen as the peaks with broader widths than the experimental resolution. High resolution experimental data are eagerly waited to clarify the origin of the broad peaks.

   Though we should wait for the detailed theoretical works including configuration mixing of the core excited states to fully investigate the $^{51}_{\Lambda}$V spectrum, a model calculation with a relatively large ls splitting for the ^{51}V(γ,K$^+$)$^{51}_{\Lambda}$Ti reaction, has been carried out [37, 35]. Assuming the broad peaks are naively caused by a large ls splitting (V_{so} = 2 MeV), the $[\pi f_{7/2}^{-1} \otimes \Lambda d_{5/2}]6^-$ and $[\pi f_{7/2}^{-1} \otimes \Lambda d_{3/2}]5^-$ states, which are spin-orbit partners, are expected to be split by more than 1 MeV. The calculated spectrum (Fig. 15) indicates that these states can be simultaneously populated by the (e, e'K^+) reaction and they could be separated with the high energy resolution of the HKS.

Since nuclei in this mass region are well described by shell-model wave functions, it is expected that comparison between experimental data and theoretical calculations have less ambiguities. We have a good chance to investigate the single-particle nature of a Λ hyperon and also investigate the splitting of the single particle states not only in the s and p orbits but also in the d orbit.

3. **^{89}Y(e,e'K$^+$)$^{89}_{\Lambda}$Sr reaction**

   As mentioned already, $^{89}_{\Lambda}$Y is the Λ hypernucleus studied with the best statistics in the medium-heavy mass region by the (π^+, K^+) reaction. As seen in Fig. 4, splitting of these peaks were observed in addition to the major shell peak structure. As an extension of the ^{51}V(e,e'K$^+$)$^{51}_{\Lambda}$Ti reaction, (e, e'K^+) spectroscopy to this heavier mass region has a great potential, though background rate is expected to be higher. With heavier targets, we can investigate better not only ls splitting of these states by the ΛN interaction, but also single-particle nature of a Λ hyperon deeply bound in a nucleus. Therefore, we also propose to conduct an exploratory run with the ^{89}Y target to examine feasibility of extending (e,e'K$^+$) hypernuclear spectroscopy to the heavier mass region.

4. **^{6,7}Li(e,e'K$^+$)$^{6,7}_{\Lambda}$He and ^{10,11}B(e,e'K$^+$)$^{10,11}_{\Lambda}$Be reactions**

   The p-shell Λ hypernuclei have been intensively studied both experimentally and theoretically.

   Recently, there is an increasing interest in the $\Lambda - \Sigma$ coupling that is a source of ΛNN three-body force and it is especially important in high-density neutron matter [29, 36]. It naturally plays a more significant role in the neutron-excess Λ hypernuclei and it is indispensable to spectroscopically study structure of p-shell Λ hypernuclei for various isospins. It was suggested that a bump structure could appear above the threshold in the ^{7}Li(e,e'K$^+$)^{7}He reaction due to the $\Lambda - \Sigma$ coupling. The systematic measurement of the neutron-excess hypernuclei in the ^{6,7}Li(e,e'K$^+$)$^{6,7}_{\Lambda}$He and ^{10,11}B(e,e'K$^+$)$^{10,11}_{\Lambda}$Be reactions will provide valuable information on the the $\Lambda - \Sigma$ coupling.

   It should also be noted here that the (e, e'K^+) reaction has an advantage over meson induced reactions, that small and thin, enriched targets can be used due to the small beam size at the target. The ^{10,11}B

targets of 100 mg/cm^2 thickness have been specially prepared with a double-stage sintering method.

4 Experimental setup and expected performance

In this section, we describe the proposed experimental setup and also the expected performance of the spectrometer system which is evaluated based on the experience of E89-009 and the currently commissioning E01-011.

4.1 General configuration

As we mentioned, we propose two configurations for the experiment, namely,

A) HKS + ENGE + existing Splitter (Fig. 14), and

B) HKS + new HES + new Splitter (Fig. 16).

The configuration A consists of 1) the HKS spectrometer for the kaons, 2) ENGE spectrometer for the scattered electron and 3) the splitter as the running E01-011 experiment. In Fig. 17, a plan view of the spectrometer system installed in Hall C is shown. The system fits in the space between the HMS-SOS pivot and the G0 detector system as we are using the system for the running E01-011 experiment (Fig. 18).

The configuration B adopts the same configuration as the configuration A, but the ENGE electron spectrometer and the splitter are replaced by a newly designed High resolution Electron Spectrometer (HES) and a new larger splitter to accept a beam with higher energy.

In the following subsections, each spectrometer will be explained.

4.2 High resolution Kaon spectrometer (HKS)

General specifications of the HKS spectrometer are given in Table. 2. The HKS is designed to achieve simultaneously 2×10^{-4} momentum resolution and 16 msr solid angle acceptance with the splitter. The HKS is placed rotated horizontally by 7 degrees with respect to the beam to avoid zero degree positive particles, mostly positrons. The solid angle is more than 16 msr over the momentum region of 1.2 GeV/$c \pm 12.5\%$, as designed.

The detector system for HKS is summarized in Table 3. As seen in Table 7, HKS singles rate is dominated by pions, whose rate will be up to a

few MHz. In order to achieve efficient pion rejection rate as high as 10^{-4}, three layers of aerogel Čerenkov counters with refractive index of 1.055 were installed. For the proton rejection, two layers of water Čerenkov counters doped with a wavelength shifter were used so that the Čerenkov counter has good efficiency for the wide range of incident angles. Time resolution of as good as 80 ps is a goal for the time-of-flight scintillators. By having the good time resolution, we plan to minimize the distance between the two time-of-flight wall so that a large solid angle and smaller kaon decay loss are achieved. The tracking chambers of HKS have high rate capability and accept the rate up to a few MHz. Those detectors were all commissioned in the running E01-011 experiment.

Table 3: Detectors for the E01-011 experiment

Nomenclature	Size	Comments
Drift chamber		
HDC1	$30^H \times 120^W \times 2^T cm$	xx'uu'(+30 deg)vv'(-30 deg)
		5 mm drift distance
HDC2	$30^H \times 120^W \times 2^T cm$	xx'uu'(+30 deg)vv'(-30 deg)
		5 mm drift distance
Time of flight wall		
HTF1X	$30^H \times 125^W \times 2^T cm$	7.5^W cm $\times$ 17-segments, H1949
HTF1Y	$30^H \times 125^W \times 2^T cm$	3.5^W cm $\times$ 9-segments, H1949
HTF2X	$35^H \times 170^W \times 2^T cm$	9.5^W cm $\times$ 18-segments, H1949
Čerenkov counter		
HAC1	$46^H \times 169^W \times 31^T cm$	n = 1.055 hydrophobic aerogel
		14×5" PMT (7 seg.)
HAC2	$46^H \times 169^W \times 31^T cm$	n = 1.055 hydrophobic aerogel (1)
		14×5" PMT
HAC3	$46^H \times 169^W \times 31^T cm$	n = 1.055 hydrophobic aerogel
		14×5" PMT (2)
HWC1	$35^H \times 187.2^W \times 8^T cm$	15.6^W cm $\times$ 12-segments, H1161
		Water with wavelength shifter
HWC2	$35^H \times 187.2^W \times 8^T cm$	15.6^W cm $\times$ 12-segments, H1161
		Water with wavelength shifter (3)

(1) HAC2 will be staggered by one third segment to HAC1.

(2) HAC3 will be staggered by one third segment to HAC2.

(3) HWC2 will be staggered by a half segment to HWC1.

4.3 ENGE spectrometer for configuration A

The ENGE spectrometer which was used in E89-009 is installed as a spectrometer to analyze the scattered electron momentum. However, as already mentioned, the spectrometer will be tilted vertically by about 8 degrees (Fig. 19), which was not the case in the previous E89-009 experiment.

Table 4: Detectors for the ENGE spectrometer

Nomenclature	Size	Comments
	Honeycomb drift chamber	
EDC	$12^H \times 100^W \times 30^T cm$	xx'uu'xx'vv'xx' 5mm drift (uu',vv' $\pm$30 deg)
	Hodoscope	
EHOD1	$12^H \times 100^W \times 1^T cm$	4^W cm $\times$ 25-segments, H7195
EHOD2	$12^H \times 100^W \times 1^T cm$	4^W cm $\times$ 25-segments, H7195
EHOD3	$12^H \times 100^W \times 2^T cm$	12^W cm $\times$ 1-segment, H1949

The detectors used at the ENGE are summarized in Table 4. Contrary to the E89-009 case, the position measurement at the focal plane is not sufficient to achieve good momentum resolution for the ENGE spectrometer, and thus tracking of the electrons is necessary as explained later. The electron rate at the detector is only a few MHz even with 30μA and 100mg/cm^2 target ; it is 2 orders of magnitude smaller than the case of E89-009, in which the beam intensity was limited by this bremsstrahlung electron rate at the ENGE detectors even with 50 times weaker beam and 5 times thinner target.

The optics of the combined system of the Splitter plus the tilted ENGE spectrometer shows a similar general features about focal plane geometry and momentum dispersion as the original untilted geometry used in E89-009. Introducing the tilted angle with respect to the horizontal plane, however, the momentum correlates to all the focal plane parameters, x, x', y, and y', where the x' and y' are the in-plane and out-of-plane angles, respectively. Therefore, a full tracking including both position and angular measurements is necessary. The honeycomb cell structured drift chamber was newly constructed for this purpose. Its position resolution is about 150 μm (RMS) and the angular resolution is about 1 mr (RMS). With a central momentum about 316 MeV/c, the mass resolution contribution of the ENGE spectrometer is about 90 keV (FWHM), which is equivalent or less

comparing to the other contributions. As a timing and trigger counter, a segmented scintillation hodoscope array is used as the E89-009 experiment. The hodoscope is improved to have a better timing resolution of 100 ps, and thus better signal /accidental separation can be performed.

It should be noted again that all detectors for the ENGE spectrometer were commissioned during the running E01-011 experiment.

4.4 High-resolution electron spectrometer (HES) for configuration B

The configuration B is more flexible for the acceptable beam energy than the configuration A, however, it requires to introduce a new high-resolution electron spectrometer (HES) which can momentum-analyze electrons as high as 1.0 GeV/c.

The collaboration has already started the design and construction of the HES and the new splitter.

The HES consists of Q-Q-D magnets and it is basically smaller version of the HKS (Figs. 21-24). Table 5 shows its basic parameters. The central momentum for the HKS is fixed as 1.2 GeV/c, and thus, the central momentum of the HES should be adjusted once the primary electron beam energy is decided. Therefore, the scattered electron emission angle and the installation position of HES depends on the primary beam energy (Fig. 20).

The "tilt method" will be applied to the HES as we introduced to the ENGE spectrometer. The tilt angle depends on the e' momentum, and thus the HES support system should have an adjustable mechanism (Fig. 25). Since we do not expect to change the beam energy during the experiment, a simple shimming mechanism is sufficient for this purpose.

Increasing e' momentum, the scattering angles of the corresponding Mϕller electrons become smaller. Therefore, we have a change to make the tilt angle smaller, where the virtual photon flux is larger, to the limit of the e' detector operation. Detailed analysis of the running E01-011 experiment will supply information how small tilt angle is feasible for the proposing experiment.

The detector package of the scattering electron spectrometer is basically the same as the ENGE detector, but it will be improved for the HES. The HES has a larger gap, and thus a larger drift chamber is necessary. Plastic scintillator hodoscopes are also renewed to cover larger area. Detector parameters are summarized in Table 6. Drift chamber structure is the same as the ENGE drift chamber except for its size; the readout electronics and

analysis techniques are already established in the running E01-011 experiment. Therefore, the development of the detector package is expected to be straightforward.

Table 5: Parameters of the HES spectrometer

Configuration	Q-Q-D and horizontal 50° bend
Central momentum	0.6 - 1.0 GeV/c (depends on beam energy)
Momentum acceptance	larger than $\pm$ 100 MeV/c
Momentum resolution ($\Delta p/p$)	2×10^{-4}
Electron detection angle	Horizontal : 0 degrees
	Vertical : 4.5 - 10 degrees (depends on beam energy)
Solid angle	> 10 msr with the new splitter
Maximum magnetic field	1.6 T (normal conducting magnet)

Table 6: Detectors for the HES spectrometer

Nomenclature	Size	Comments
	Drift chamber	
HEDC	$20^H \times 150^W \times 40^T cm$	Honeycomb cell structure, xx'uu'vv'xx'uu'vv'xx'
	Hodoscope	
HEHOD1	$20^H \times 4^W \times 1^T cm$	35 segmentation
HEHOD2	$20^H \times 4^W \times 1^T cm$	35 segmentation staggered with HEHOD1

4.5 Singles rates

Count rates in HKS and ENGE spectrometers were estimated as follows:

1. π^+ and proton rates in HKS were calculated for 1.2 GeV/c particles emitted at an angle of 7 degrees with using the EPC code. The results were normalized by the experimental values measured in E89-009 for a carbon target at 2.2 degrees.
2. Quasifree kaon production cross section was assumed to scale as $A^{0.8}$.
3. Electron rate in ENGE was evaluated by two methods, one by EGS code and the other code by Lightbody, which agreed more or less to each other.

4. Pion rate in ENGE was calculated based on the EPC code, and normalized by the same factor used for hadron rates in HKS.

As seen in Table 7, singles rate of HKS is dominated by positive pions, while that for ENGE is by electrons. It should be noted that we expect the positron rate in HKS is low since we setup HKS at an angle off 0 degrees. The singles rate of the ENGE hodoscope is expected almost two orders of magnitude less than that of E89-009. With this rate, the hardware coincidence between electron arm and kaon arm can form good triggers.

With 100 mg/cm^2 carbon and 30μA beam in the running E01-011 experiment, total rates in the HKS and ENGE are respectively measured as 0.5 MHz and 2.3 MHz; they are consistent with the above estimation.

Table 7: Singles rates

Target	Beam Intensity (μA)	HKS e^+ rate (MHz)	HKS π^+ rate (kHz)	HKS K^+ rate (Hz)	HKS p rate (kHz)	ENGE e^- rate (MHz)	ENGE π^- rate (kHz)
^{7}Li	30	-	330	423	118	0.6	2.2
^{10}B	30	-	417	394	126	0.9	2.8
^{12}C	30	-	416	380	148	1.0	2.8
^{51}V	30	-	366	285	119	2.7	3.1
^{89}Y	30	-	366	255	119	4.1	3.1

4.6 Resolution of excitation energy spectra

The following factors contribute to the total resolution of the experiment:

1. HKS momentum resolution
   With a Monte Carlo simulation, the momentum resolution of the HKS was estimated to be 75 keV/c (RMS) with a spatial resolution of 200μm for the drift chambers.

2. Beam momentum resolution
   Assuming 1×10^{-4}, it will be 180 keV/c (FWHM) for 1.8 GeV/c beam. For higher momentum beam, the better accuracy is required to maintain beam uncertainty contribution less than 180 keV/c.

3. ENGE momentum resolution
   For vertical and horizontal resolutions of the chamber as 150μm, the momentum resolution of the ENGE spectrometer is estimated to be 93 keV (FWHM).

4. Kinematical broadening due to uncertainty of the K^+ scattering angle
   The uncertainty of the K^+ emission angle is dominated by the multiple scattering through the materials between the target and the chambers (uncertainty due to the spatial resolution of the chambers are less than 0.2 mrad). Contribution of the following materials are taken into account: the target (100 mg/cm^2), vacuum windows (kevlar 0.008", mylar 0.005"), helium bag (100 cm) and chambers (mylar 0.0045", argon 5.08 cm @ STP).

   Total uncertainty of the K^+ angle was estimated to be 3.3 mrad (RMS) for the carbon target. This angular uncertainty corresponds to 152 keV (FWHM) ambiguity to the ${}^{12}_{\Lambda}$B mass.

5. Momentum loss in the target
   The momentum loss in the target was calculated for 1.2 GeV/c K^+ assuming Vavilov distribution. The whole momentum loss in the target will contribute the mass resolution without any correction. The average momentum loss of 1.2 GeV/c K^+ in the carbon 100 mg/cm^2 was 195 keV/c which corresponds to the energy resolution of 180 keV(FWHM).

The results are summarized in Table 8. Present proposed experimental setup will achieve the resolution 300-400 keV (FWHM).

Table 8: The energy resolution of the HKS system

Item	Contribution to the resolution (keV, FWHM)			
Target	Li	C	V	Y
HKS momentum			190	
Beam momentum			≤ 180	
ENGE or HES momentum			93	
K^+ angle	230	152	36	20
Target (100 mg/cm^2)	≤ 170	≤ 180	≤ 148	≤ 138
Overall	$\leq$ **400**	$\leq$ **360**	$\leq$ **320**	$\leq$ **310**

4.7 Background and signal/noise ratios

One of the major sources of background in the proposed setting that facilitates detection of very forward particles is electrons associated with bremsstrahlung and Mϕller processes. The "tilt method" offers us 50 times

more hypernuclear yield and a factor of 10 better signal to noise ratio compared to the E89-009 setup.

Electron and hadron rates were estimated as given in Table 7 for the beam current of 30 μA and the target thickness of 100 mg/cm^2. It shows that 2.8 MHz of the electron background in the ENGE spectrometer which placed with 8 degrees to the beam axis (1.851 GeV electron beam, 100 mg/cm^2 carbon target), and it is consistent with the measured value of 2.3 MHz in the running E01-011 experiment. Kaon single rate for the HKS spectrometer was estimated to be 380 Hz as shown in Table 7. With a coincidence window of 2 ns, we have accidental coincidence rate as:

$$N_{ACC} = (2.8 \times 10^6 \mathrm{Hz}) \cdot (2 \times 10^{-9} \mathrm{sec}) \cdot (380 \mathrm{Hz}) \sim 2.1/\mathrm{sec}.$$

Assuming that the accidental coincidence events spread uniformly over the energy matrix (ENGE 149 MeV $\times$ HKS 240 MeV), the largest background per bin (100 keV) projected on the hypernuclear mass spectrum will be 9 $\times$ 10^{-4} /sec. A typical hypernuclear (^{12}C target) event rate will be 48.4 / (100 nb/sr) / h = 1.3 $\times 10^{-2}$ / (100 nb/sr) / sec as shown in Table 9.

Table 9: Expected hypernuclear production rates in the (e,e'K$^+$) reaction (Target thickness 100 mg/cm^2)

Target	beam Intensity (μA)	Counts per 100nb/sr $\cdot$ hour	Qfree K$^+$ in HKS(Hz)
^{7}**Li**	15	41	210
^{11}**B**	30	53	390
^{12}**C**	30	48	380
^{51}**V**	30	11	285
^{89}**Y**	30	6.5	255

5 Yield estimate and requested beam time

The expected yield of the hypernuclear states are evaluated based on the E89-009 result for $^{12}_{\Lambda}$B ground state in the ^{12}C(e,e'K$^+$)$^{12}_{\Lambda}$B reaction. The proposed "tilt method" is expected to realize more than 50 times hypernuclear yield rate gain. It is partly because we can use higher intensity beams and thicker targets and partly because the kaon

spectrometer has a larger solid angle acceptance and better momentum matching with the electron spectrometer.

The cross sections of the hypernuclear states for the targets, ^{7}Li,^{12}C,^{51}V have been calculated by Motoba and Sotona for the present experimental conditions [35, 37]. They are listed in Table 10.

It is noted, however, the calculated cross sections could vary by a factor of 2-5 depending on the choice of model parameters for the elementary reaction, the hypernuclear potentials, the configuration of the states and so on. In the present yield estimate, the cross sections were normalized assuming the cross section of the ^{12}C(e,e'K^{+})$^{12}_{\Lambda}$B reaction for the ground state doublet is 100 nb/sr.

Table 10: Cross sections of $^{7}_{\Lambda}$He, $^{12}_{\Lambda}$B and $^{51}_{\Lambda}$Ti calculated by DWIA [37]

Target	Hypernucleus	Hypernuclear configuration	Cross section (nb/sr)
^{7}Li	$^{7}_{\Lambda}$He	$s_{1/2}$	28
		$s_{1/2}$	11
		$p_{3/2}$	15
		$s_{1/2}$	52
^{12}C	$^{12}_{\Lambda}$B	$s_{1/2}$	112
		$p_{3/2}$	79
		$p_{1/2}$	45
^{51}V	$^{51}_{\Lambda}$Ti	$s_{1/2}$	18
		$p_{3/2}$	41
		$p_{1/2}$	26
		$d_{5/2}$	52
		$d_{3/2}$	48
		$1s_{1/2}$	16
		$f_{7/2}$	32
		$f_{5/2}$	38

With the ENGE spectrometer as the electron spectrometer (Configuration A), we request the commissioning time of 4 days. In the case that the newly constructed HES spectrometer is installed, we request additional commissioning beam time of 4 days.

Tuning the spectrometer system coupled with the tilted ENGE spectrometer will be carried out with a CH_2 target using the Λ and Σ peaks. The $^{12}_{\Lambda}$B ground state peak will be used combined with the above Λ and Σ

Table 11: Requested beam time. Number in parenthesis means requested commissioning time when the HES spectrometer is used.

	Target	Hypernucleus	Number of days	Number of hours
Spectrometer commissioning and calibration			4 (8)	96 (192)
Data taking				
	^{6,7}Li,^{10,11}B	$^{6,7}_{\Lambda}$He,$^{10,11}_{\Lambda}$Be	4	96
	^{51}V	$^{51}_{\Lambda}$Ti	14	336
	^{89}Y	$^{89}_{\Lambda}$Sr	4	96
Total for data taking			22	**528**
Grand Total			26 (30)	**624 (720)**

Table 12: Requested beam conditions

	Configuration A	Configuration B
Typical beam energy	1.8 GeV	2.1 - 2.5 GeV
Typical beam current	30 μA	30 μA
Beam energy stability	$\leq 1 \times 10^{-4}$	$\leq 7 \times 10^{-5}$

peaks for tuning the spectrometer system and for the mass calibration.

The requested data taking hours for the V target was calculated so that 400 counts for $^{51}_{\Lambda}$Ti can be accumulated, assuming 60 % efficiency for data taking and data analysis. For $^{89}_{\Lambda}$Sr, the requested beam time is only for an exploratory run. The beam times for the p-shell Λ hypernuclei are requested as well. The collaboration prepared the enriched targets of ^{6,7}Li and ^{10,11}B with the thickness of about 100 mg/cm^2 and they are ready to receive beams. We would like to decide which targets should be used in the proposed experiment, considering the progress of theoretical studies by the beam time. The requested beam times are summarized in Table 11. Requested beam conditions are listed in Table 12.

6 Schedule of the spectrometer construction and requested support

The HKS spectrometer with the detector package can be stationed at the present position or at the parking position in Hall C, but will be ready for

use without any major work anytime as far as the beam at around 1.8 GeV is delivered to Hall C.

Unless the beam at around 1.8 GeV is available, we need to install the HES spectrometer under construction for this proposed experiment. In this case, we request JLab to provide a basement support structure of the HES spectrometer and some modification of the beam dump line (DZ-EZ magnets chicane) that has capability to transport the 2.0 - 2.5 GeV beam to the dump. Although the power supply for the HES dipole will be brought by the collaboration, DC power supplies for the other magnets are requested in addition to operate the HKS spectrometer magnets..

The present schedule for the construction of the HES spectrometer is shown in Table 13. The design of the spectrometer is almost complete and some of the magnets are already under construction. It is the plan of the collaboration to ship the HES spectrometer system including the focal plane detectors from Japan to JLab in the fall of 2006 to be delivered to JLab by the end of 2006 calendar year.

Since the detectors for the HES is almost the same as those for the ENGE spectrometer, we see no difficulty to construct them and test them using cosmic rays and available accelerator beams ($eg.$ LNS-Tohoku) before we receive the beam at JLab.

7 Summary

High-resolution (e,e'K^+) spectroscopy for the two medium-heavy targets, ^{51}V and ^{89}Y, and two of the four p-shell targets, ^{6,7}Li and ^{10,11}B, has been proposed. By the proposed (e, e'K^+) spectroscopy, we intend to reveal 1) single-particle nature of a Λ hyperon by deriving single particle binding energies and widths and/or splitting of the single-particle states in the medium heavy hypernuclei; 2) splitting of higher-l single particle states in view of ΛN ls interaction and its structural origin in medium-heavy hypernuclei; and 3) characteristic structure of medium-heavy hypernuclei, $^{51}_{\Lambda}$Ti($^{89}_{\Lambda}$Sr) and neutron excess p-shell hypernuclei, $^{6,7}_{\Lambda}$He ($^{10,11}_{\Lambda}$Be).

An exploratory spectrum will be also taken for the ^{89}Y target, in order to examine the possibility to extend (e, e'K^+) hypernuclear spectroscopy to the heavier targets.

The present proposal postulates that we use the high resolution kaon spectrometer (HKS) which has been installed in Hall C for the E01-011 experiment.

Table 13: Present expected time line for the HES spectrometer construction and installation. It is emphasized, however, the collaboration can run the proposed experiment with the setup used in the running E01-011 experiment.

April, 2004 - March, 2005	
	Design of the spectrometer system
	Contract with a magnet manufacture
	Construction of Q1 and Q1
	Design of detectors
April, 2005 - March, 2006	
	Construction of the dipole magnet
	Design and construction of the HES focal plane drift chambers
	Design and construction of the hodoscope of HES
April, 2006 - March, 2007	
	Completion of the detector construction
	Assembly of the detector system at JLab
	Assembly and test of the spectrometer magnet at JLab
	Transportation of the HES magnets from Tohoku U. to JLab (before the end of 2006)
	Installation of the spectrometer system in the Hall

The collaboration presented two options for an electron spectrometer; one is the ENGE spectrometer being used in E01-011 and the other the high-resolution electron spectrometer (HES).

The HKS-ENGE combination allows us to carry out the proposed experiment anytime but requires about 1.8 GeV beam energy. The HES is now under construction by the Tohoku group with the budget of MEXT, Japan and will be ready for use at the beginning of 2007. The HES option can accept much wider range of the beam energy.

The proposal is fully based on the success of the E89-009 experiment carried out in the spring of 2000 and also the experience during the commissioning of the E01-011 experiment in June, 2005. Once the proposed experiment is successfully performed, we envision that the next stage of the hypernuclear physics program by the (e,e'K^+) reaction will be fully explored taking advantage of the high-quality high-power CW electron beams at Jefferson Laboratory as 1) Λ hypernuclear spectroscopy for targets as heavy as Pb; 2) Intensive high quality spectroscopy of light Λ hypernuclei; and also 3) Open the doorway to coincidence experiments.

References

[1] B. Povh, Prog. Part. Nucl. Physics **18** (1987) 183.

[2] R. Chrien and C. Dover, Ann. Rev. Nucl. Part. Sci. **39** (1989) 113.

[3] H. Bandō, T. Motoba, J. Žofka, Int. J. Mod. Phys. **21** (1990) 4021.

[4] O. Hashimoto and H. Tamura, Prog. Part. Nucl. Physics in printing (2005).

[5] M. M. Nagels *et al.*, Phys. Rev. D **15** (1977) 2547; Phys. Rev. D **20** (1979) 1633; P. M. Maessen *et al.*, Phys. Rev. C **40** (1989) 2226; Th.A. Rijken, V.G.J. Stokes and Y. Yamamoto, Phys. Rev. C **59** (1999) 21.

[6] B. Holzenkamp *et al.*, Nucl. Phys. **A500** (1989) 458; K. Holinde, Nucl. Phys. **A547** (1992) 245c.

[7] Y. Yamamoto *et al.*, Prog. Theor. Phys. Suppl. **118** (1994) 361.

[8] H. Bandō, T. Motoba and Y. Yamamoto, Phys. Rev. **C31** 265 (1985).

[9] A. Likar, M. Rosina and B. Povh, Z. Phys. **A324** 35 (1986).

[10] T. Yamazaki
Proc. KEK Int. Workshop on Nuclear Physics in the GeV region, KEK Report 84-20(1984) p.3.

[11] M. Danysz and J. Pniewski, Phil. Mag. **44** (1953) 348.

[12] C. Milner $et.\ al.$, Phys. Rev. Lett. **54** (1985) 1237;
P. H. Pile *et al.*, Phys. Rev. Lett.**66** (1991) 2585.

[13] O. Hashimoto *et al.* Il Nuovo Cimento **102** 679 (1989).

[14] T. Fukuda *et al.*, Nucl. Instr. Meth. **A361** (1995) 485.

[15] T. Hasegawa *et al.*, Phys. Rev. **C53** (1996) 1210.

[16] O. Hashimoto, Hyperfine Interactions **103** (1996) 245.

[17] H. Hotchi *et al.*, Phys. Rev. C **64** (2001) 044302.

[18] 89Y spectrum T. Nagae, Nucl. Phys. **A670** (2000) 269c-272c.

[19] S. Ajimura *et al.*, Phys. Rev. Lett. **86** (2001) 4255; H. Kohri *et al.*, Phys. Rev. C **65** (2002) 034607.

[20] H. Akikawa *et al*, Phys. Rev. Lett. **88** (2002) 082501.

[21] T. Motoba, Private communication, 2003.

[22] O. Hashimoto, Proc. Int. Workshop on Strangeness Nuclear Physics, Seoul (World Scientific 1999), p. 116.

[23] T. Tamura *et al.*, Phys. Rev. Lett. **84** (2000) 5963.

[24] T. Kishimoto, Talk at HYPJLAB99, December 5-7, 2000, Hampton, Virginia, USA.

[25] H. Tamura, Talk at HYP2000, October 21-26, 2000, Torino, Italy.

[26] M. Ukai *et al.*, Phys. Rev. Lett. **93** (2004) 232501.

[27] K. Tsushima, K. Saito, J. Haidenbauer, A.W. Thomas, Nucl. Phys. **A630** (1998) 691.

[28] C.B. Dover, Proc. Int. Symp. on Medium Energy Physics, p.257, Beijing (World Scientific, Singapore, 1987).

[29] Y. Akaishi, T. Harada, S. Shinmura and Khin Swe Myint, Phys. Rev. Lett. **84** (2000) 3539.

[30] T. Hasegawa *et al.*, Phys. Rev. Lett. **74** (1995) 224.

[31] C.B. Dover, L. Ludeking and G.E. Walker, Phys. Rev. **C22** 2073 (1980).

[32] H. Bandō and T. Motoba, Prog. Theor. Phys. **76** 1321 (1986).

[33] T. Motoba, H. Bandō, R. Wünsch and J. Zofka, Phys. Rev. **C38** 1322 (1988).

[34] T. Motoba, M. Sotona and K. Itonaga, Prog. Thor. Phys. Suppl. No. 117 (1994) 123.

[35] M. Sotona $et\ al.$, Proceedings of Mesons and Light Nuclei '98, p. 207. 1998.

[36] S. Shinmura, Khin Swe Myint, T. Harada and Y. Akaishi, J. Phys. G **28** (2002) L1.

[37] T. Motoba, Private communication, 1997.

Figures

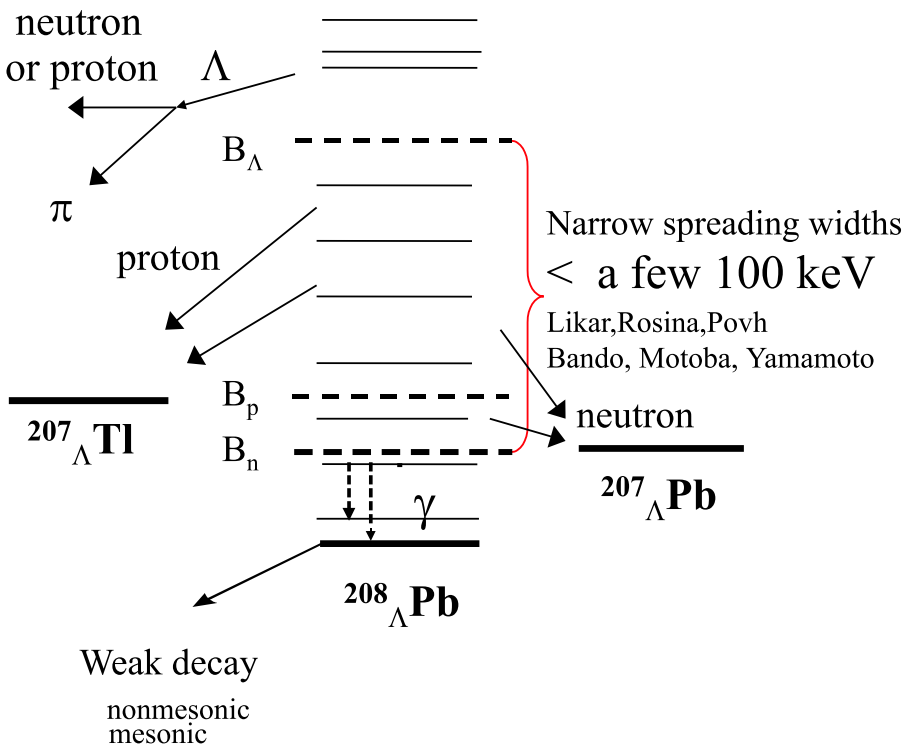

Figure 1: Λ hypernuclear states and their decay modes.

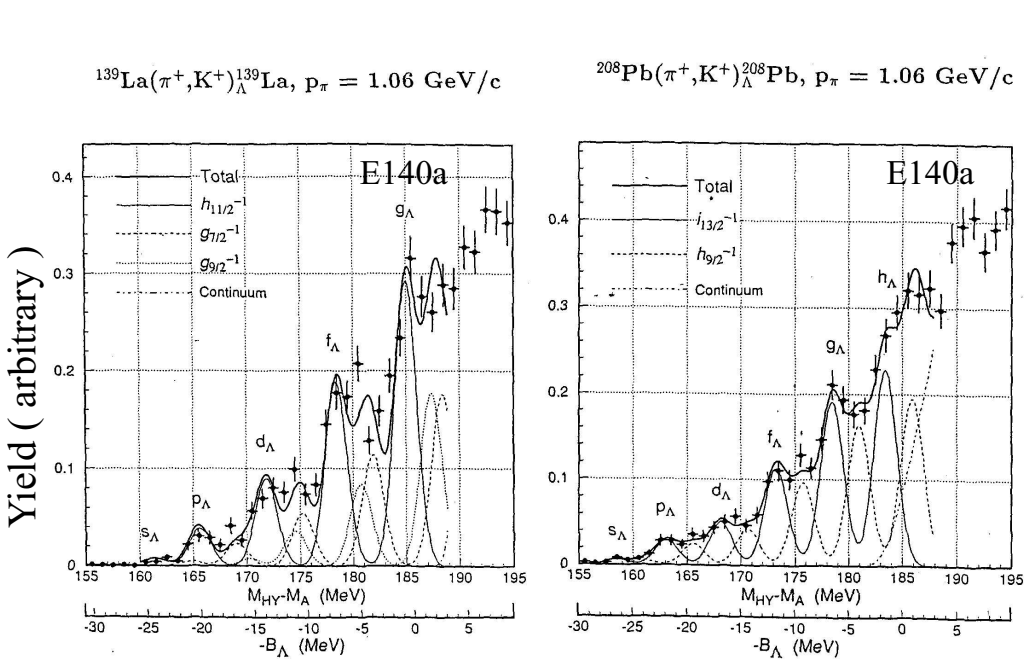

Figure 2: Excitation energy spectrum of $^{139}_{\Lambda}$La and $^{208}_{\Lambda}$Pb measured with the SKS spectrometer of KEK-PS by the (π^+, K^+) reaction.

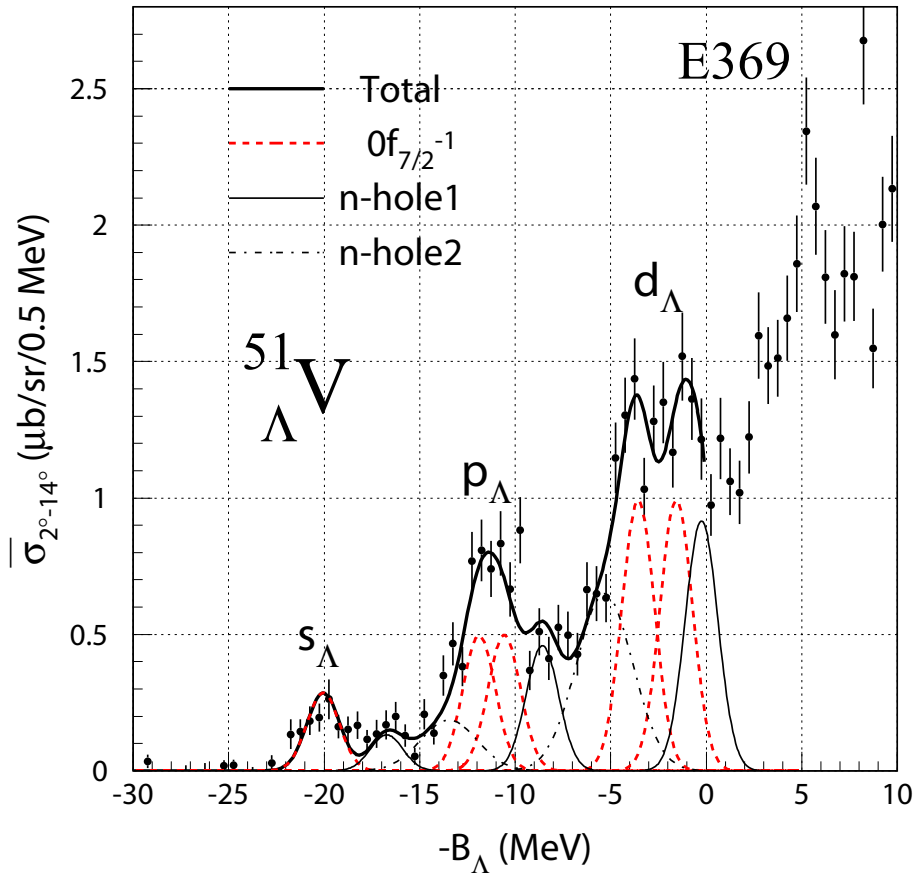

Figure 3: Missing mass spectrum of $^{51}_{\Lambda}$V(KEK E369) [17].

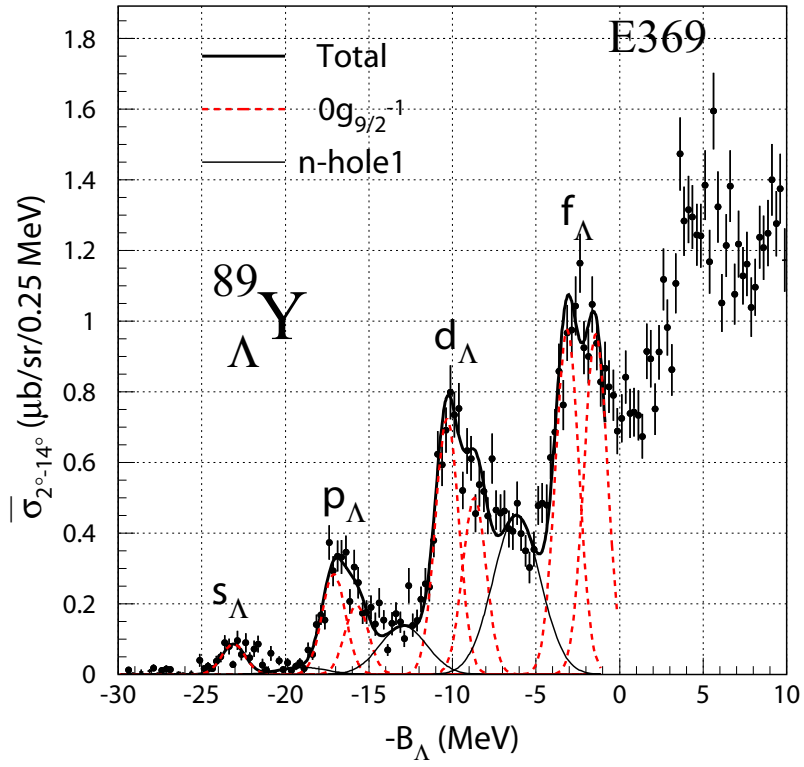

Figure 4: Missing mass spectrum of $^{89}_{\Lambda}$Y(KEK E369) [17].

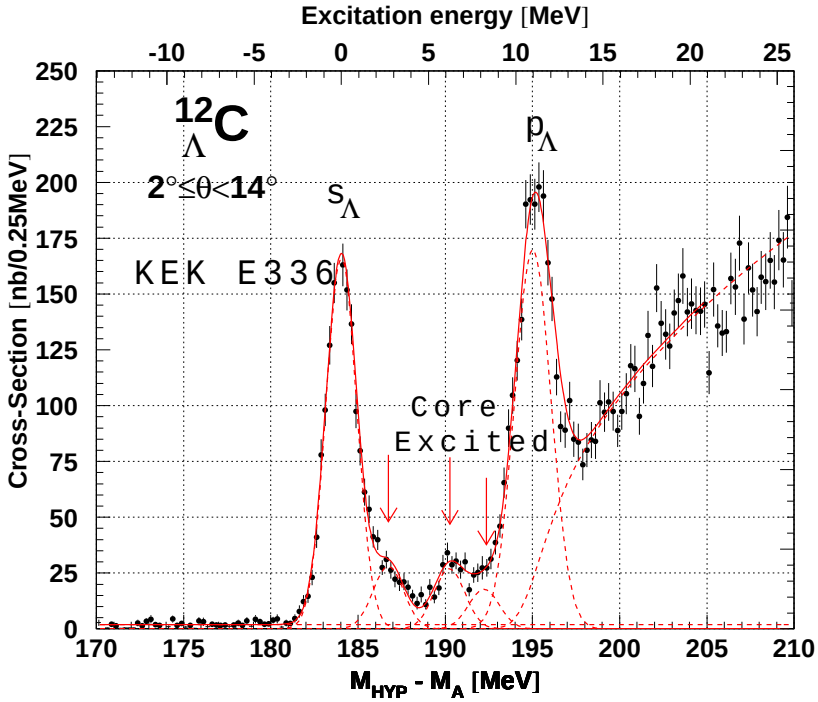

Figure 5: Excitation energy spectrum of $^{12}_{\Lambda}$C measured with the SKS spectrometer of KEK-PS by the (π^+, K^+) reaction.

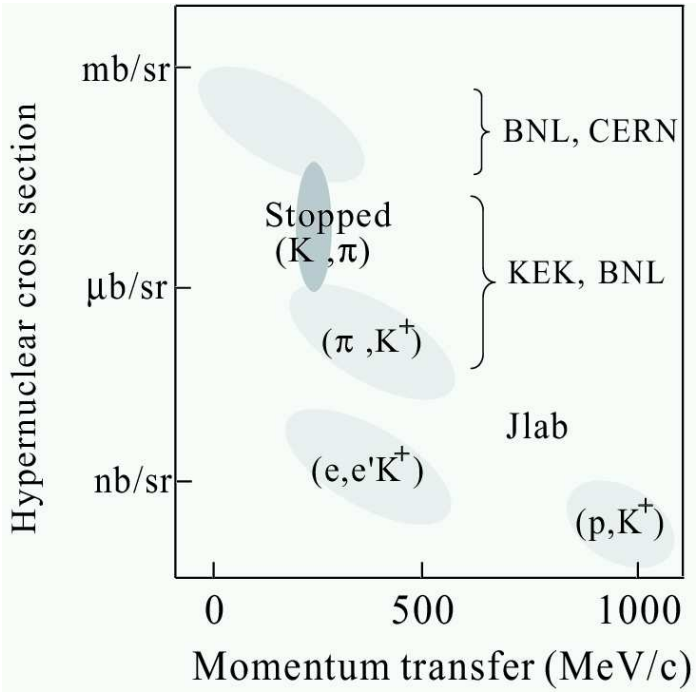

Figure 6: Hypernuclear production cross section for typical reactions vs. momentum transfer.

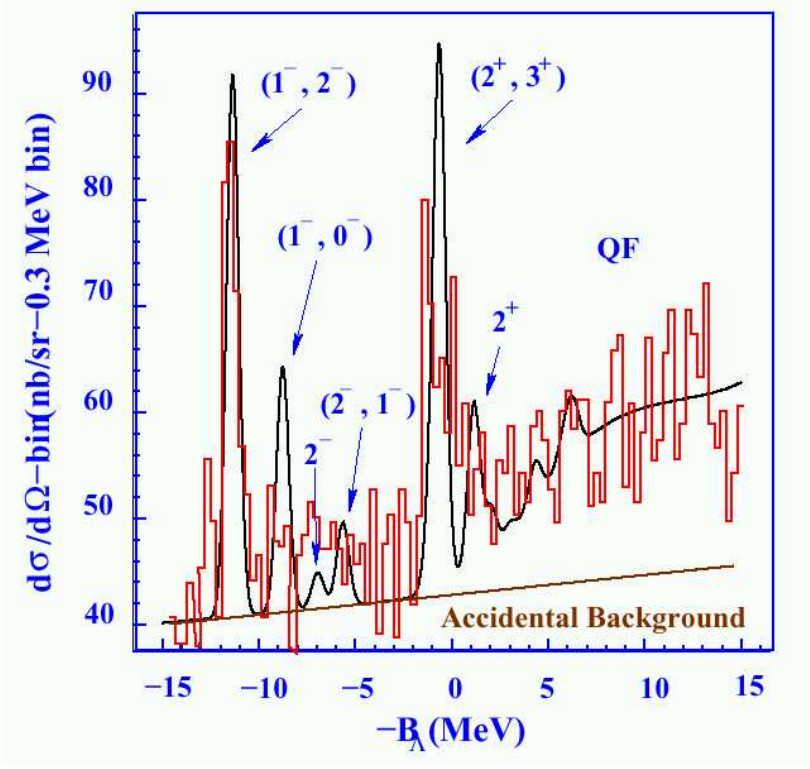

Figure 7: Excitation energy spectrum measured in the E89-009 experiment

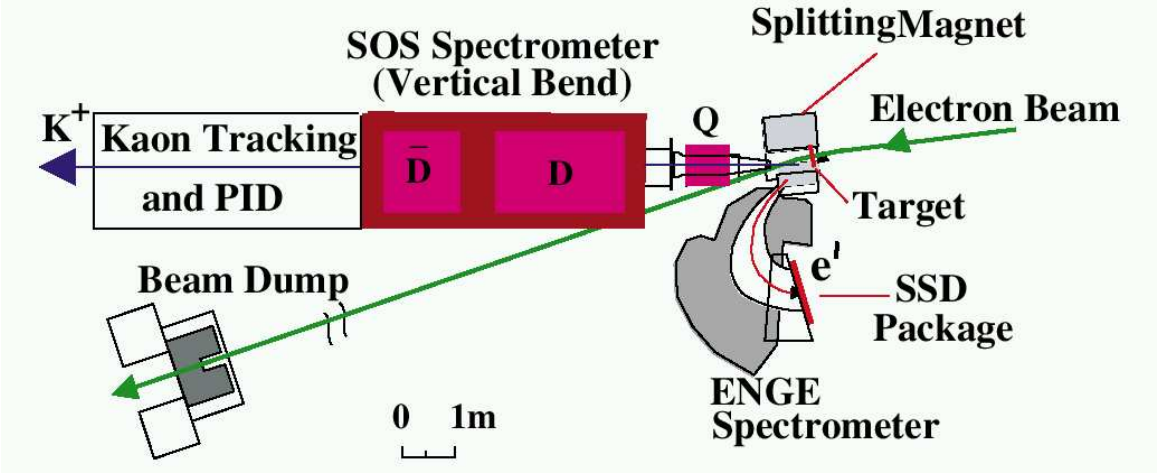

Figure 8: A schematic view of the E89-009 setup.

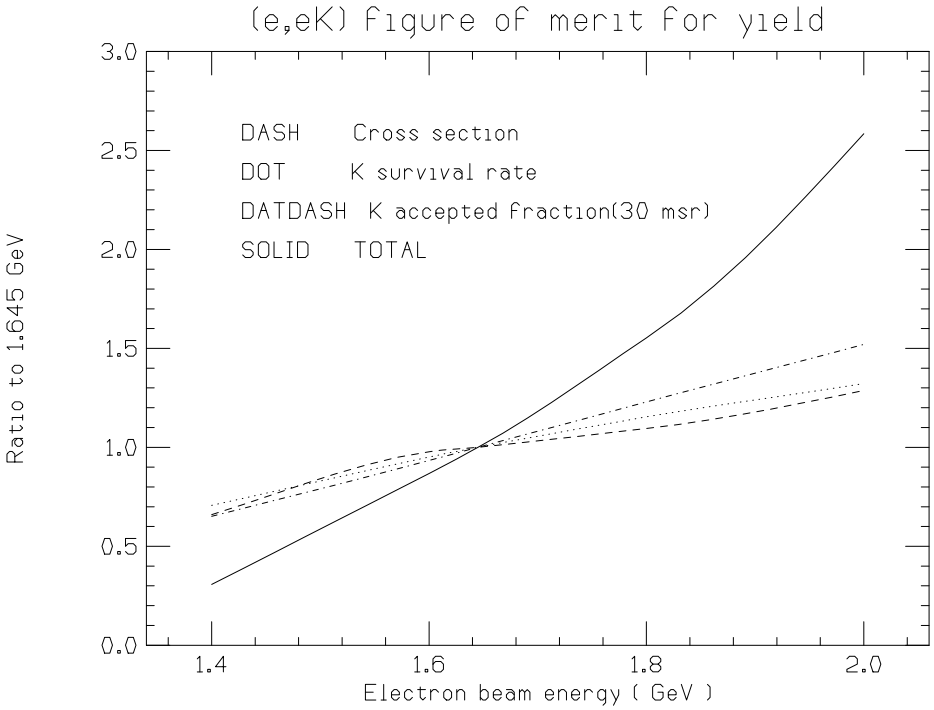

Figure 9: Hypernuclear yield of ${}^{12}_{\Lambda}\mathrm{B}_{gr}$ as a function of the beam energy assuming scattered electrons are measured at E_e = 0.285 GeV.

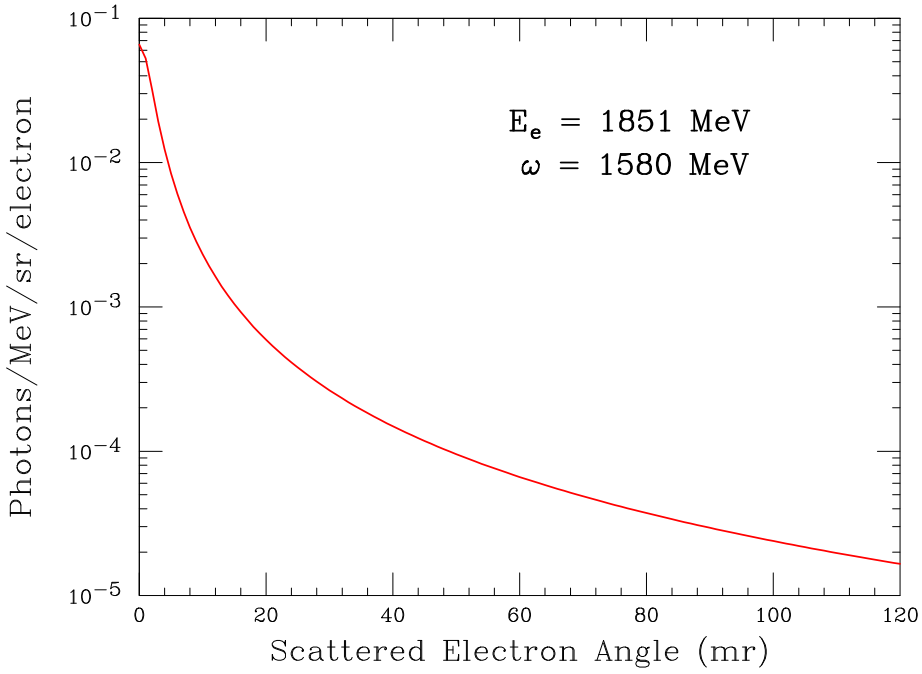

Figure 10: Angular distribution of virtual photons with the ^{12}C target

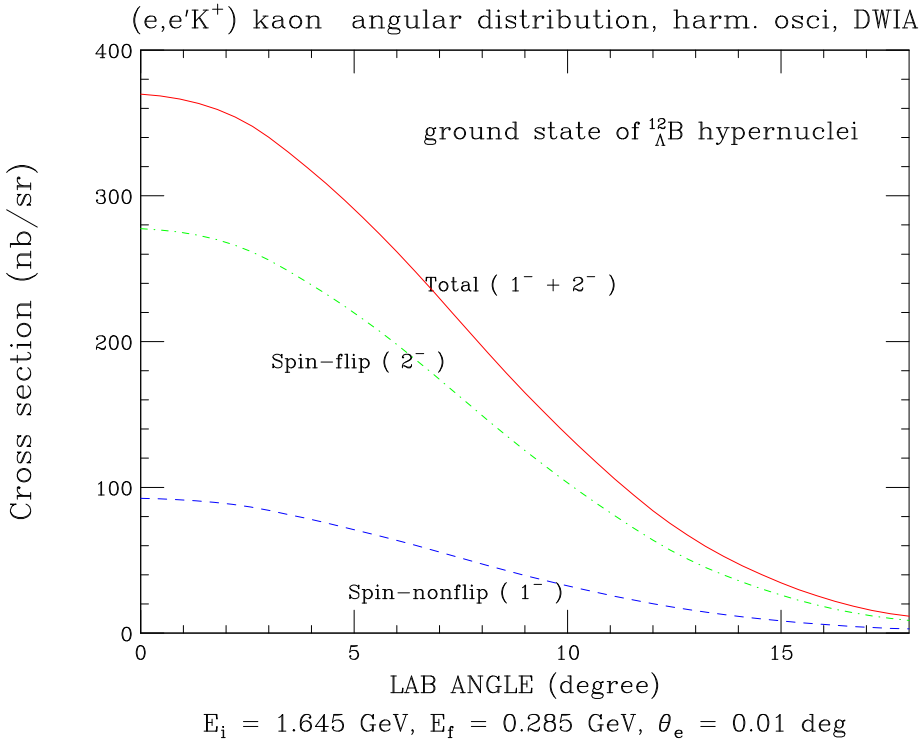

Figure 11: Angular distribution of kaon in the ^{12}C(e,e'K$^+$)$^{12}_{\Lambda}$B reaction.

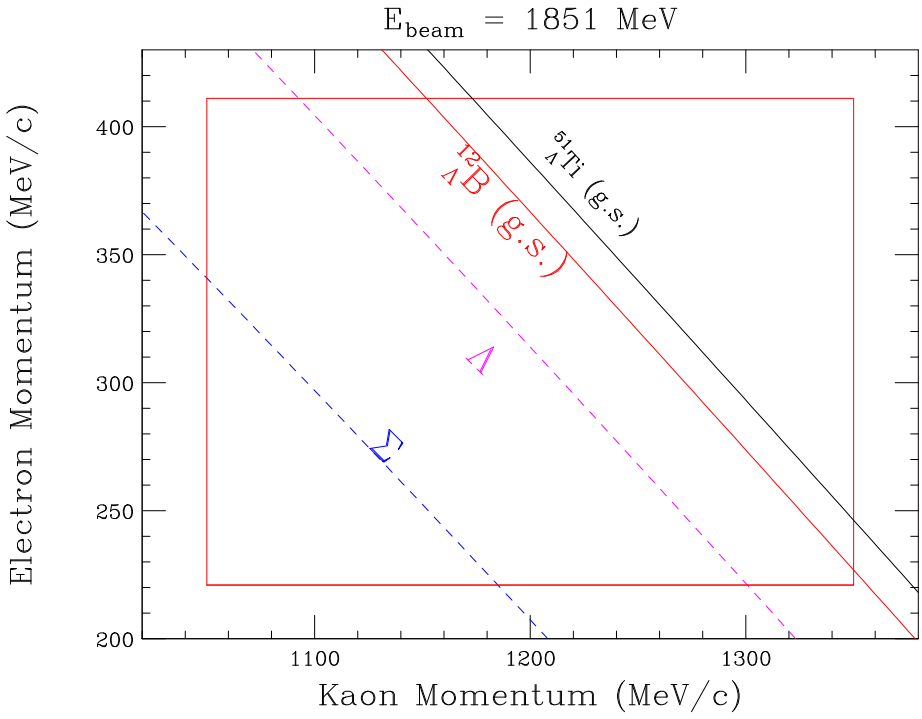

Figure 12: Momentum correlation between kaon arm (detection angle, 7 degrees in horizontal plane) and electron arm (scattering angle, 4.5 degrees in vertical plane) for hyperons and hypernuclei production reaction. Electron energy of 1851 MeV was assumed.

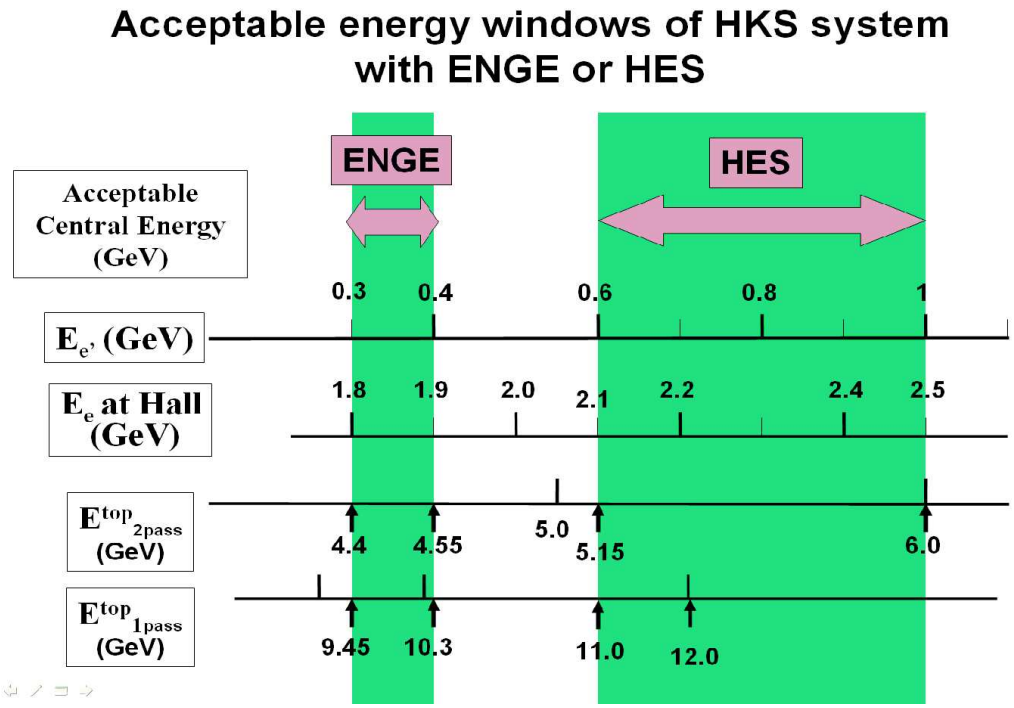

Figure 13: Acceptable energy windows of the HKS system with ENGE or HES. With the ENGE option, the beam energy at Hall C should be 1.8-1.9 GeV. It corresponds to the CEBAF top energy of 4.40-4.55 (9.45-10.3) GeV if Hall C uses 2 passes (1 pass) beam. HES enables the top CEBAF energy to be 5.0-6.0 or 10.8-12.0 GeV and thus it is more flexible.

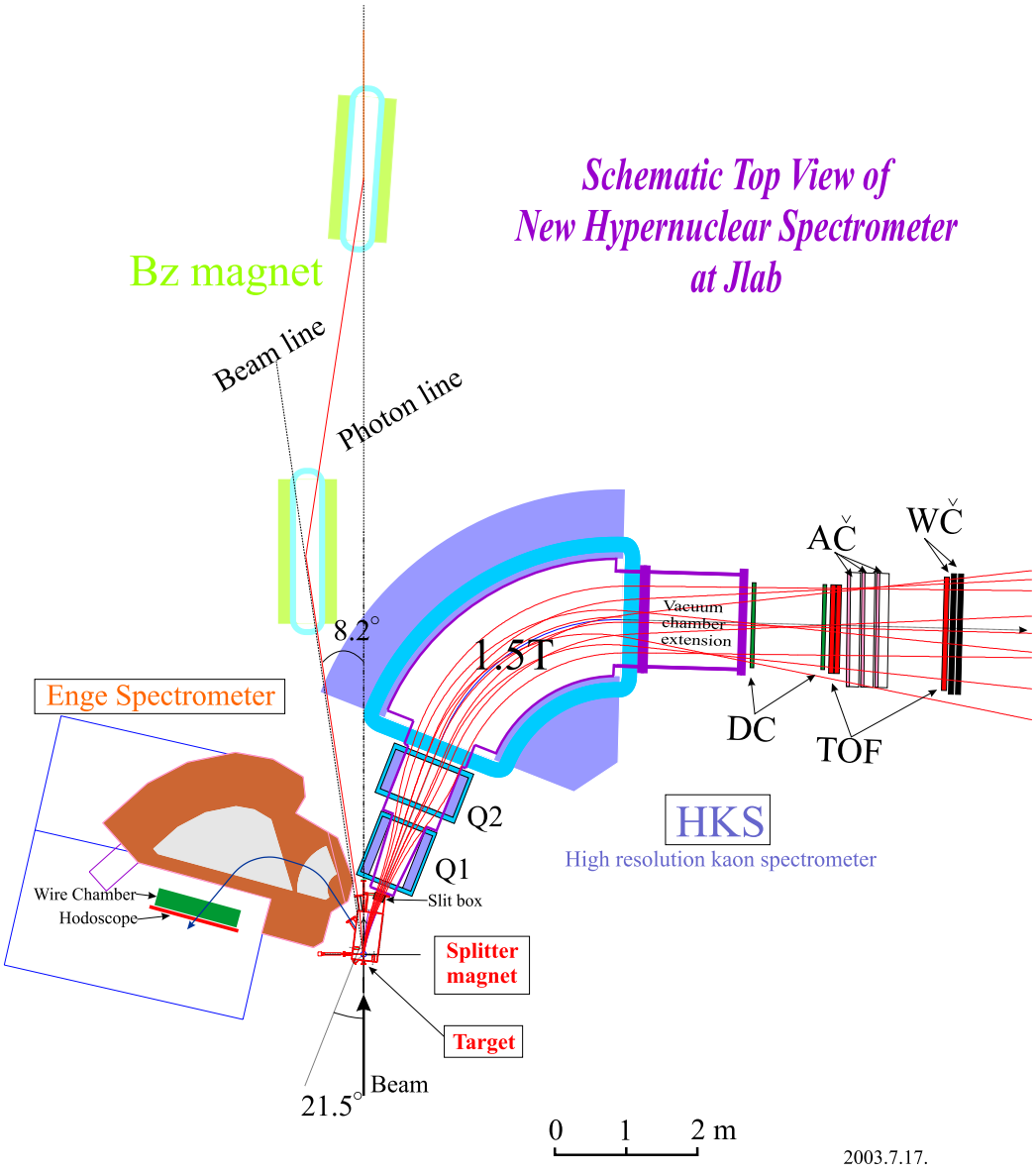

Figure 14: Plan view of the high-resolution kaon spectrometer (HKS) and ENGE spectrometer for the proposed experiment.

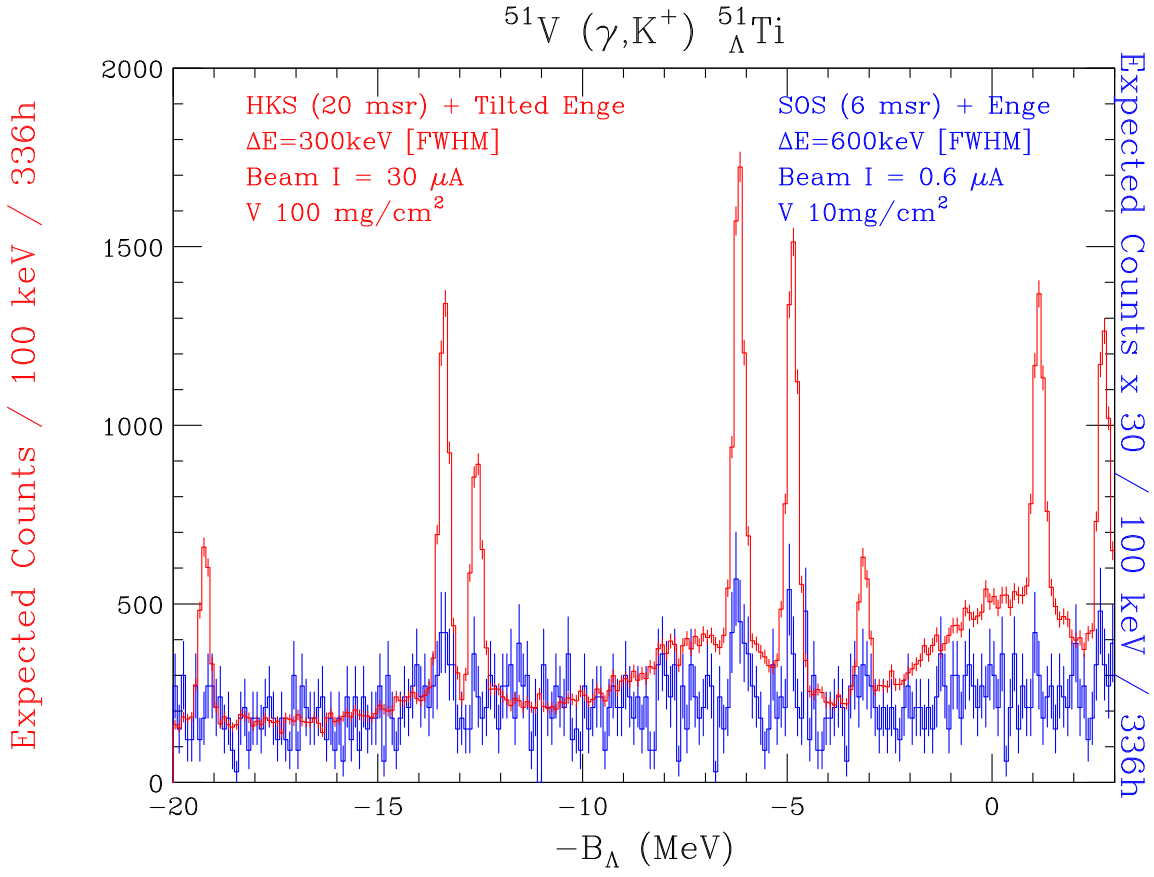

Figure 15: Simulated spectrum of the ^{51}V(e,e'K$^+$)$^{51}_{\Lambda}$Ti reaction to be observed by the HKS in the proposed beam hours.

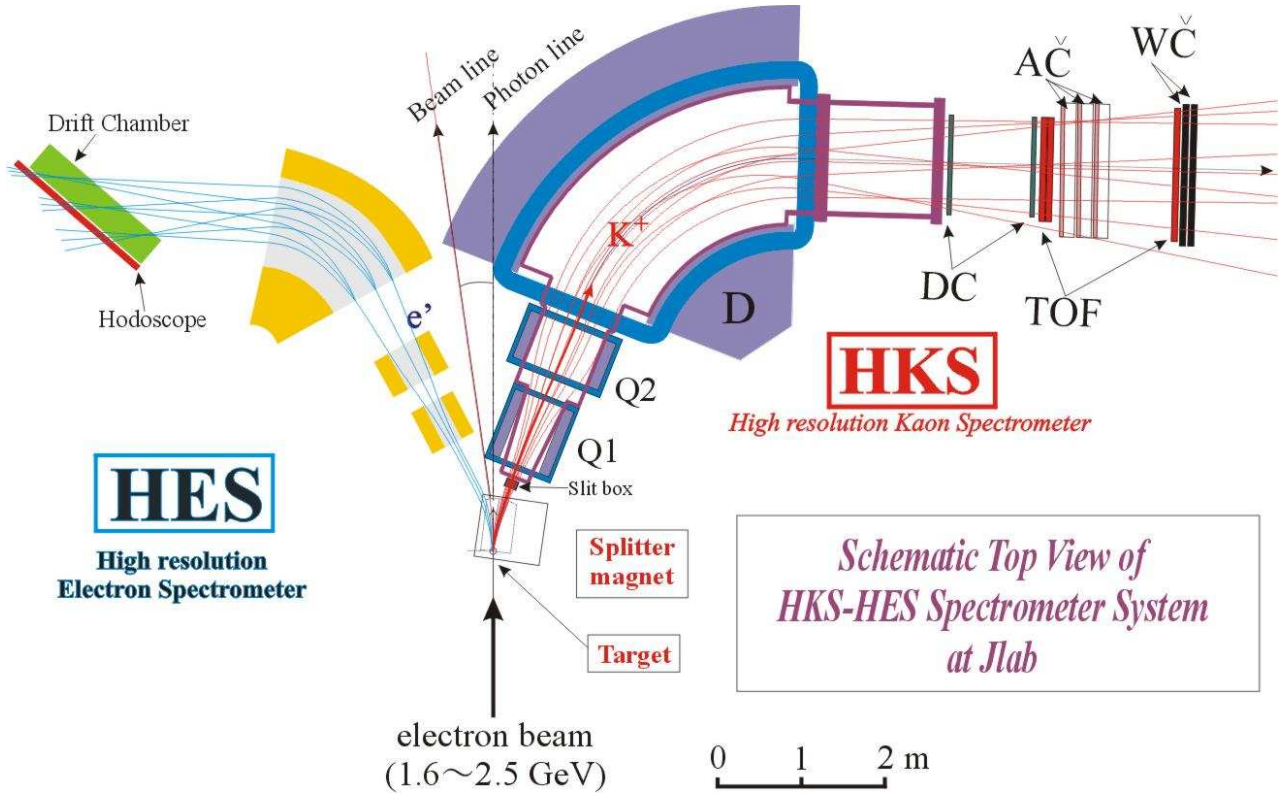

Figure 16: The HKS-HES setup (configuration B). Adequate chicane magnets should be placed to guide unused deflected electron beam to dump as the running E01-011 does.

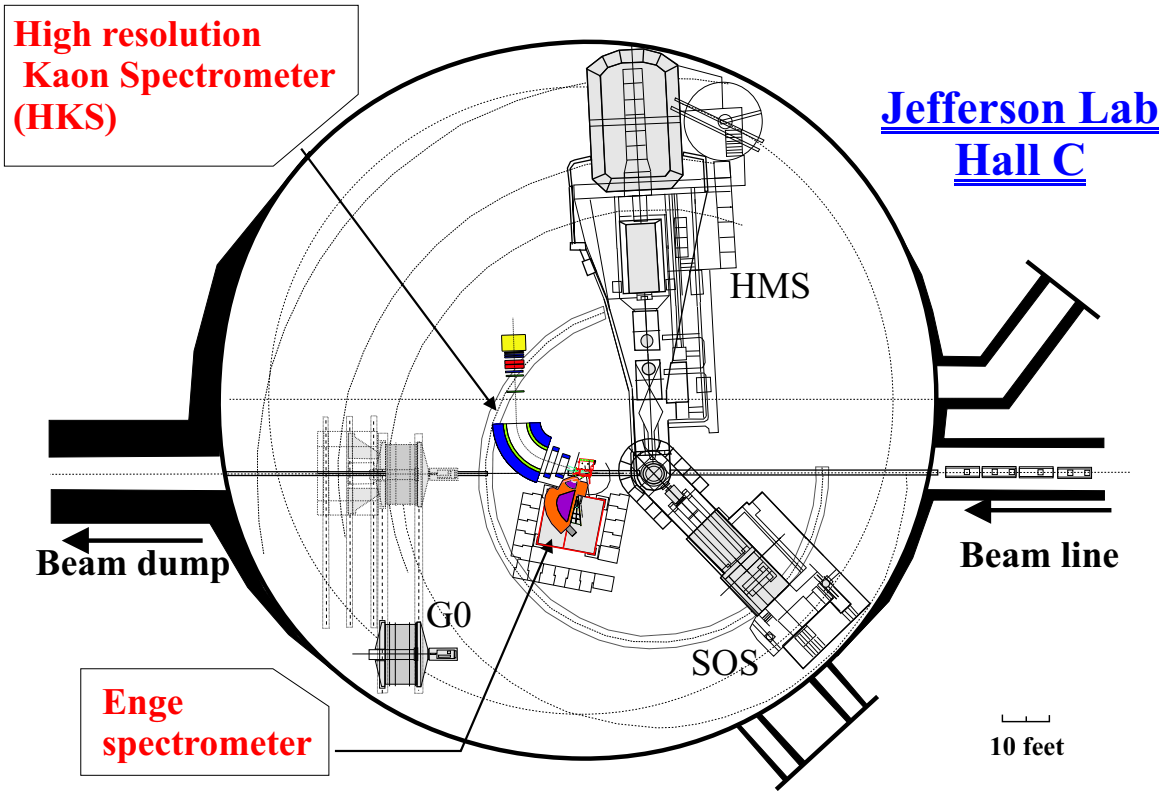

Figure 17: Expected Hall C setup of the HKS and ENGE spectrometer. The installation can be compatible with the G0 setup.

Figure 18: The HKS-ENGE setup installed in Hall C.

Figure 19: The ENGE spectrometer installed with a vertical tilt angle of 8 degrees in Hall C.

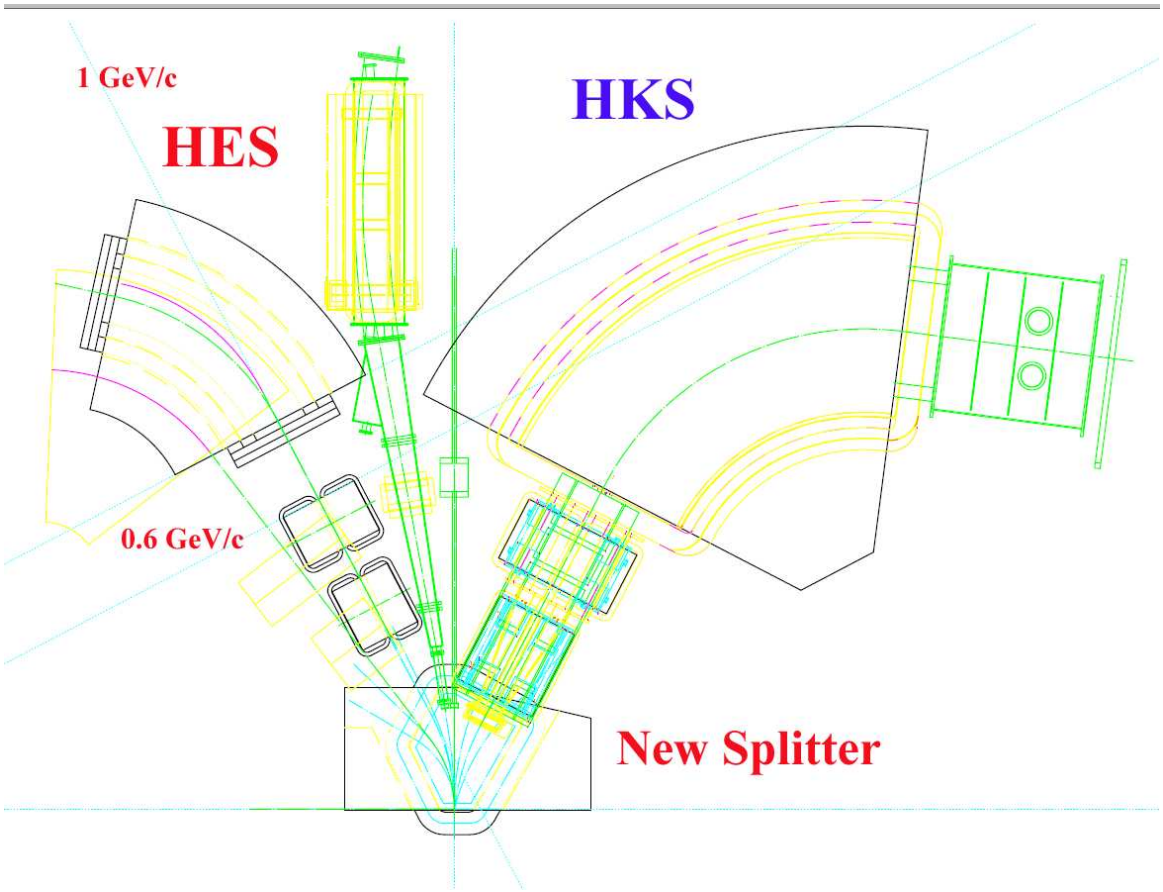

Figure 20: The HES spectrometer with a new splitter and HKS. The HES position depends on the scattering electrons' central momentum, since the magnetic fields of the splitter and HKS are unchanged.

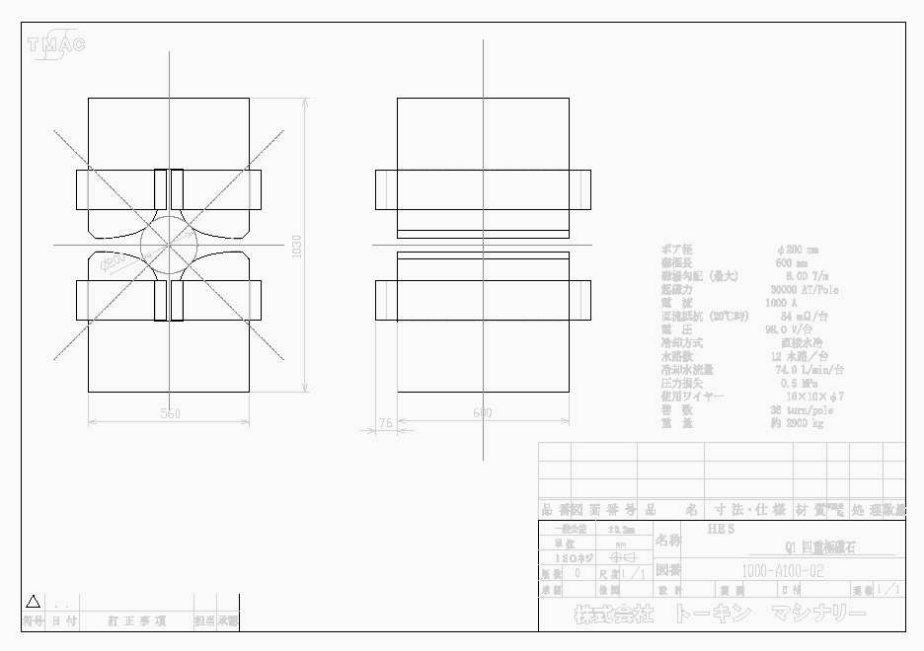

Figure 21: The preliminary design of the HES Q1 magnet.

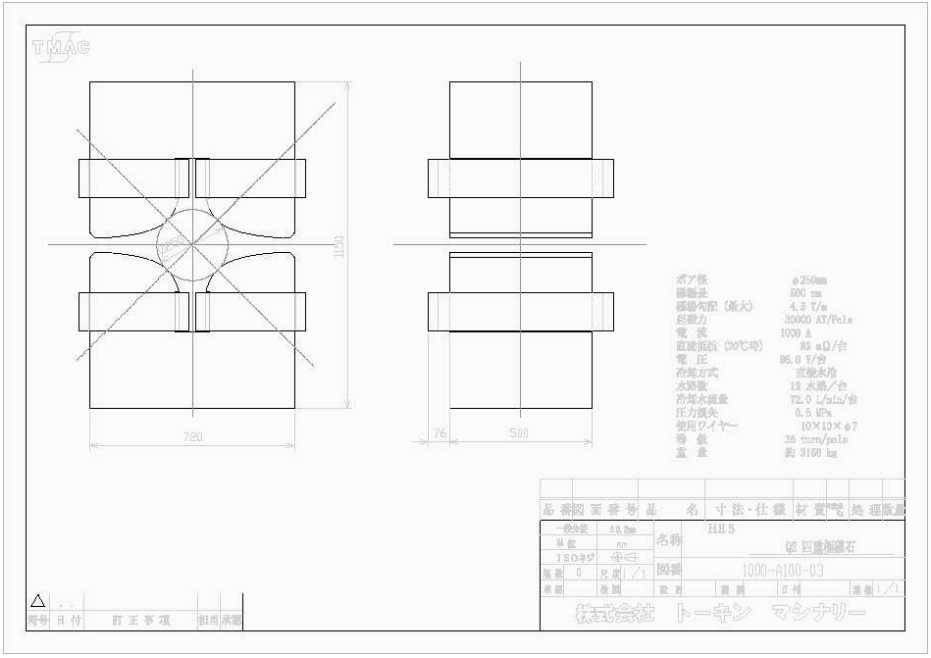

Figure 22: The preliminary design of the HES Q2 magnet.

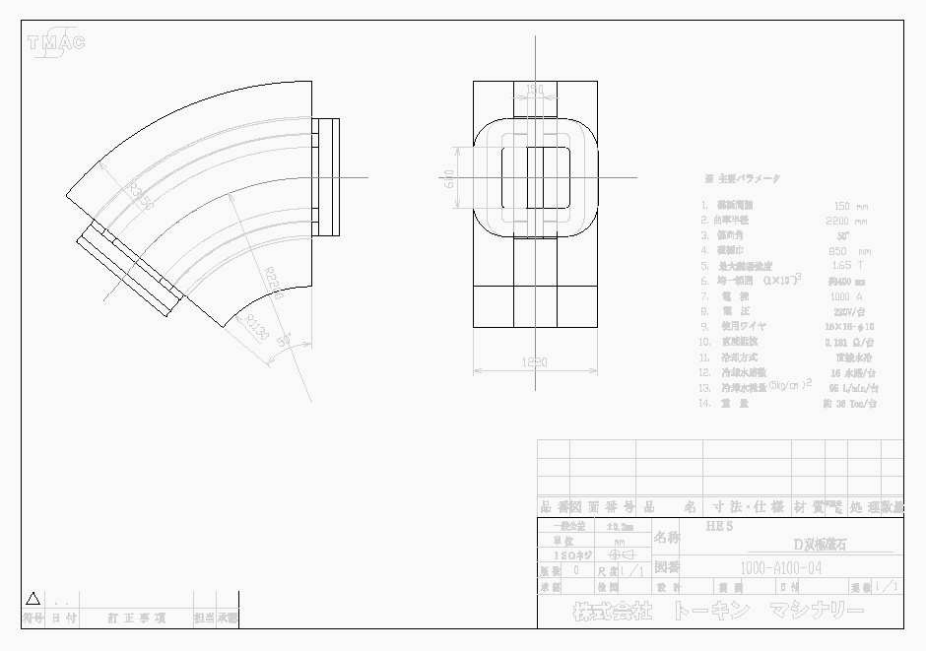

Figure 23: The preliminary design of the HES D magnet.

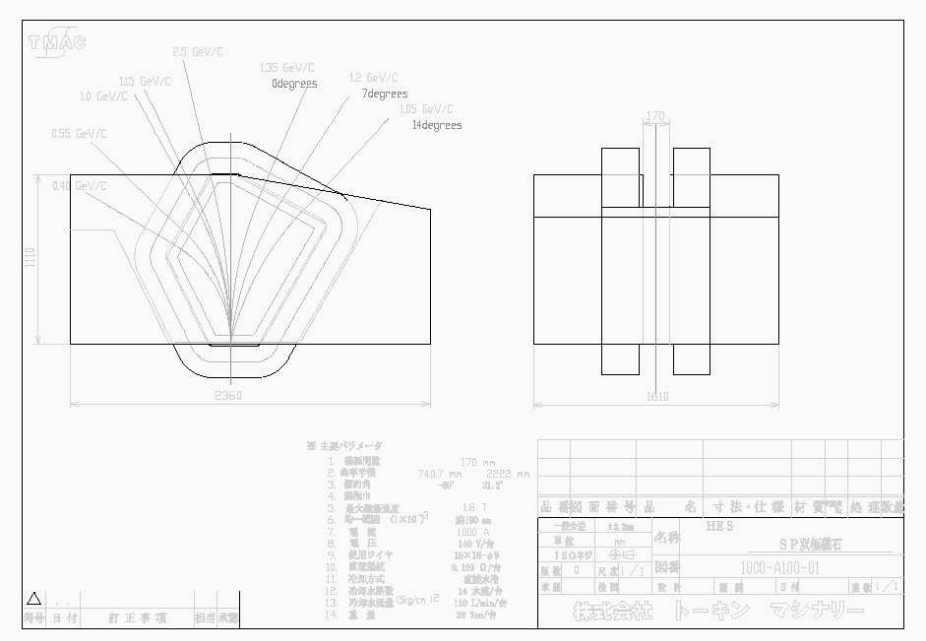

Figure 24: The preliminary design of the new splitter magnet.

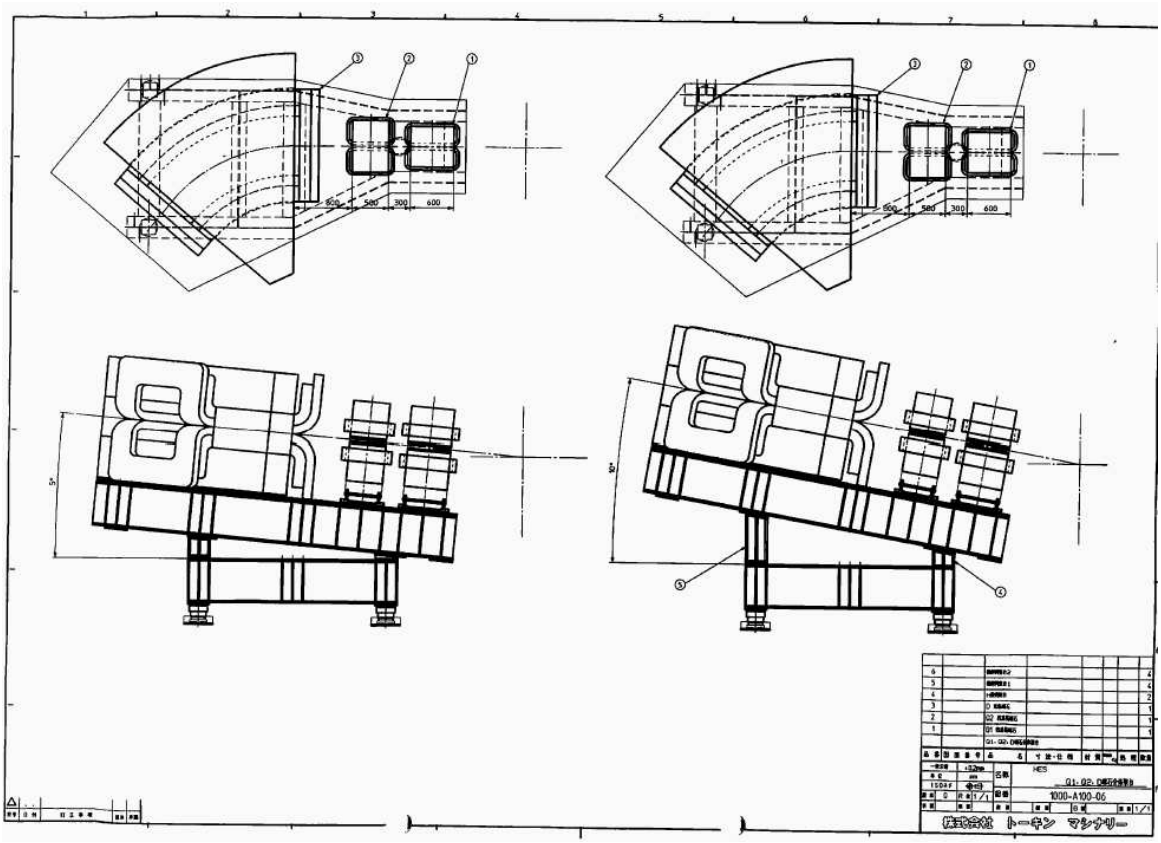

Figure 25: The “tilt method” will be also applied to the HES. The tilt angle will be optimized to the central momentum. It can be realized by changing the shim under the HES.